IOP PUBLISHING INVERSE PROBLEMS

Inverse Problems **25** (2009) 045005 (34pp) doi:10.1088/0266-5611/25/4/045005

Background velocity estimation with cross correlations of incoherent waves in the parabolic scaling

Josselin Garnier[1] **and Knut Sølna**[2]

[1] Laboratoire de Probabilités et Modèles Aléatoires & Laboratoire Jacques-Louis Lions, Université Paris VII, 2 Place Jussieu, 75251 Paris Cedex 5, France
[2] Department of Mathematics, University of California, Irvine, CA 92697, USA

E-mail: garnier@math.jussieu.fr and ksolna@math.uci.edu

Received 2 June 2008, in final form 12 January 2009
Published 17 February 2009
Online at stacks.iop.org/IP/25/045005

Abstract

In this paper the incoherent waves reflected by a random medium in the parabolic regime are considered. The case in which the medium has anisotropic three-dimensional rapid random fluctuations and one-dimensional slow variations is analyzed. First, it is shown how the second-order statistics of the reflected wave is determined by the slow spatial variations of the background velocity, the scattering coefficient and the absorption coefficient of the medium via a system of transport equations. Next, it is shown how observations of the time-dependent intensity, spatial radius and spectral radius of the reflected wave can be used to invert this system in order to reconstruct the parameters of the medium. Finally, it is shown that the analytic framework set forth can also be used to analyze the time dynamics of weak localization.

(Some figures in this article are in colour only in the electronic version)

1. Introduction

The parabolic regime for wave propagation in random media describes many important physical situations, in geophysics [3], in optics [4, 14], in underwater acoustics [6, 15] or in medical imaging [16]. This regime has been extensively studied and the properties of the transmitted wave are well known. Much less is known about the reflected waves, because the reflected waves are incoherent and have small amplitudes in this regime. However, in many situations (in imaging or remote sensing) only the reflected waves can be measured, and it is therefore important to study them and to show how information about the medium can be extracted from the incoherent reflections. In [8] we showed that the second-order moments of the reflected wave follow a system of transport equations in the case in which the background velocity and impedance are constant, the medium is non-absorbing and the random fluctuations of the medium are spatially stationary. In this paper we continue this

analysis, we now assume that the medium is absorbing and has two types of fluctuations: on the one hand, one-dimensional, deterministic, slow and smooth variations, and on the other hand, anisotropic three-dimensional, random and rapid fluctuations. In this case the heterogeneities in the medium do not create coherent reflected waves, the reflected waves are incoherent. We develop the generalized system of transport equations in this inhomogeneous case, and we show how the second-order statistics of the reflected waves depend on the slow variations of the parameters of the medium. With this result we show that it is possible to image the medium from the observation of the incoherent reflected waves, in the sense that it is possible to invert the system of transport equations from the observation of the cross correlations of the reflected wave and to reconstruct the one dimensional, slowly varying components of the parameters of the medium.

Inverse problems in which one seeks to detect large-scale features of the environment from multiply scattered waves have been addressed in a number of configurations, in particular in [1, 5, 7, 13, 20]. In these papers, the authors address the situation in which the slow background variations and the rapid random fluctuations of the medium are one dimensional. In our paper, we discuss the case in which the slow background variations are one dimensional and the rapid random fluctuations are three dimensional. This setting is particularly relevant for background velocity estimation in geophysics. The formulation we use here is similar to that used in [1], the information about the large-scale features of the medium is contained in the cross moments of the reflected wave, which are solutions of transport equations in which the background velocity appears. The inverse problem then consists in inverting the system of transport equations.

In addition to solving the inverse problem, the analysis of the second-order statistics of the reflected wave allows us to study carefully the enhanced backscattering phenomenon. Enhanced backscattering (or weak localization) refers to the phenomenon that when an incoming plane wave is applied with a given incidence angle, the mean reflected power has a local maximum in the backscattered direction, twice as large as the mean reflected power in the other directions. It was first predicted by physicists [2, 19] and then observed in several experimental contexts [11, 17, 18, 21]. In this paper we study the dynamics of weak localization. We show that the enhanced backscattering factor converges in time to 2 at an exponential rate, while the angular width of the enhanced backscattering cone decays as a power law.

The paper is organized as follows. We introduce the scaling regime and the quantities of interest in section 2, and we present the system of transport equations for the reflection operator in section 3. Then, we study systematically the second-order statistics of the reflected waves in section 4, including enhanced backscattering in section 5. We use our results in the context of imaging problems in section 6. Finally, in section 7, we carry out numerical simulations in the case in which the background velocity or the statistical properties of the microstructure is stepwise constant, and when the detection problem involves identification of the location of the interface at which the parameters change and also the parameters of the medium on either side.

2. Waves in a random medium

We consider linear acoustic waves propagating in $1+d$ spatial dimensions with heterogeneous and random medium fluctuations. The governing equations are

$$\rho(z,\boldsymbol{x})\frac{\partial \boldsymbol{u}}{\partial t}+\nabla p+\gamma(z,\boldsymbol{x})\boldsymbol{u}=\boldsymbol{F}, \qquad \frac{1}{K(z,\boldsymbol{x})}\frac{\partial p}{\partial t}+\nabla\cdot\boldsymbol{u}=0, \tag{1}$$

where p is the pressure, $\boldsymbol{u}$ is the velocity, ρ is the density of the medium, K is the bulk modulus of the medium, γ is the absorption coefficient and $(z, \boldsymbol{x}) \in \mathbb{R} \times \mathbb{R}^d$ are the space coordinates. The source is modeled by the forcing term $\boldsymbol{F}$. Here we shall focus on propagation through and reflection from a random slab occupying the interval $z \in (0, L)$ with the source $\boldsymbol{F}$ located outside of the slab, say at $z = L$. The parameterization is motivated by waves probing for instance the heterogeneous earth and one may think of z as the main probing direction. We shall refer to waves propagating in a direction with a positive z component as right-propagating waves.

The medium parameters in the random slab $(0, L)$ have two types of spatial variations: on the one hand, anisotropic three-dimensional, small, rapid and random fluctuations and on the other hand, one-dimensional, slow, and deterministic variations (those that we want to identify in the imaging problem). Outside the slab $(0, L)$ the medium is non-absorbing and has only slow and smooth variations. The medium is assumed to be matched at the boundaries $z = 0$ and $z = L$. The medium parameters can be written as

$$\frac{1}{K(z,\boldsymbol{x})} = \begin{cases} K_0^{-1}(z) & \text{if} \quad z \leqslant 0, \\ K_0^{-1}(z)\,(1+\nu_K(z,\boldsymbol{x})) & \text{if} \quad z \in (0,L), \\ K_0^{-1}(z) & \text{if} \quad z \geqslant L, \end{cases}$$

$$\rho(z,\boldsymbol{x}) = \rho_0(z), \qquad \gamma(z,\boldsymbol{x}) = \begin{cases} 0 & \text{if} \quad z \leqslant 0, \\ \gamma_0(z) & \text{if} \quad z \in (0,L), \\ 0 & \text{if} \quad z \geqslant L, \end{cases}$$

where ρ_0, K_0 and γ_0 are the deterministic smooth functions that describe the one-dimensional slow variations of the medium and the random field $\nu_K(z, \boldsymbol{x})$ models the three-dimensional rapid random fluctuations. The process ν_K has zero mean and its autocorrelation function is of the form

$$C_K(z, z', \boldsymbol{x}') = \mathbb{E}[\nu_K(z+z', \boldsymbol{x}+\boldsymbol{x}')\nu_K(z, \boldsymbol{x})].$$

Note that C_K does not depend on $\boldsymbol{x}$, which means that the statistics of ν_K is stationary in the transverse direction, but C_K does depend on z. As explained in detail below we shall assume that the dependence on z is relatively slow and that the statistics is locally stationary in the longitudinal direction. We assume that the random fluctuations of the medium are smooth in $\boldsymbol{x}'$ so that C_K is at least twice differentiable at $\boldsymbol{x}' = \mathbf{0}$, with $\Delta_{\boldsymbol{x}'} C_K(z, 0, \mathbf{0}) < 0$. The longitudinal (respectively transverse) correlation radius l_z (respectively l_x) of the random fluctuations and the standard deviation σ can be defined by

$$\sigma^2 = \frac{1}{L}\int_0^L C_K(z, 0, \mathbf{0})\,\mathrm{d}z, \tag{2}$$

$$\sigma^2 l_z = \frac{1}{L}\int_0^L \int_{-\infty}^{\infty} C_K(z, z', \mathbf{0})\,\mathrm{d}z'\,\mathrm{d}z, \tag{3}$$

$$\frac{\sigma^2}{l_x^2} = -\frac{1}{\mathrm{d}L}\int_0^L \Delta_{\boldsymbol{x}'} C_K(z, 0, \mathbf{0})\,\mathrm{d}z. \tag{4}$$

The source is located at the surface $z = L$ and it has the form

$$\boldsymbol{F}(t, z, \boldsymbol{x}) = f_s(t, \boldsymbol{x})\delta(z - L)\boldsymbol{e}_z,$$

where $\boldsymbol{e}_z$ is the unit vector pointing in the z-direction. We denote by ω_0 the typical frequency of the source term f_s and by R_0 the diameter of its spatial support (which gives the initial beam width). The typical wavelength associated with the typical frequency ω_0 is $\lambda_0 = 2\pi c_0(L)/\omega_0$, for $c_0(L) = \sqrt{K_0(L)/\rho_0(L)}$ the background speed at $z = L$.

2.1. Scaling

We now describe the scaling regime that we consider in this paper, which ensures that both the paraxial (or parabolic) approximation and the white-noise approximation are valid. We introduce a typical propagation distance l_p, which is of the same order as the width L of the random slab:

(i) We assume that the longitudinal correlation length l_z of the medium is smaller than the transverse correlation length l_x, which is smaller than the propagation distance l_p. In geophysics we typically have $l_p \sim 10^4$ m, $l_x \sim 10^2$–10^3 m and $l_z \sim$ 1–10 m. Denoting by ε^2 the ratio between the longitudinal correlation length l_z and the propagation distance l_p, we assume that we have $l_z/l_p = \varepsilon^2$ and $l_x/l_p \sim \varepsilon$. In this regime we anticipate that the longitudinal random fluctuations of the medium can be approximated by a 'white noise'. We remark that the statistics of the medium may change on the scale say of major geological features, corresponding to the scale l_p.

(ii) We assume that the width of the beam R_0 and the transverse correlation length of the medium l_x are of the same order. In geophysics the source can be an explosion at the sea surface that generates a field which expands so that its width becomes of the order of 10^2–10^3 m at the sea bottom. Accordingly we assume that the ratio R_0/l_p is of order ε. In this regime, there is a non-trivial interaction between the transverse fluctuations of the medium and the beam.

(iii) We assume that the typical wavelength λ_0 of the source is of the same order as the longitudinal correlation length l_z. In geophysics we typically have $\lambda_0 = 10$–10^2 m. Accordingly we assume that the ratio λ_0/l_p is of order ε^2. In this regime, there is a non-trivial interaction between the longitudinal fluctuations of the medium and the beam. Moreover, the ratio of the Rayleigh length $\pi R_0^2/\lambda_0$ over the propagation distance l_p is also of order one. Since the Rayleigh length is the distance from beam waist where the beam area is doubled by diffraction in a homogeneous medium, this means that diffraction effects are expected to be of order one, which corresponds to the parabolic regime.

(iv) We assume that the amplitude of the random medium fluctuations is weak. In geophysics the fluctuations of the sound speed in the earth's crust is of the order of 10%. Accordingly we assume that $\sigma \sim \varepsilon$.

We now put the system in dimensionless form. We consider the propagation distance, l_p, as our reference distance. We denote by $\bar\rho$ and $\bar K$ a typical density and bulk modulus (for instance, the density and bulk modulus at the surface), and by $\bar c = \sqrt{\bar K/\bar\rho}$ and $\bar\zeta = \sqrt{\bar K\bar\rho}$ the corresponding speed and impedance. The evolution equations for the dimensionless variables $(\tilde p, \tilde{\boldsymbol u})(\tilde t, \tilde z, \tilde{\boldsymbol x})$ defined by

$$\boldsymbol u = \bar\zeta^{-1/2}\tilde{\boldsymbol u}, \qquad p = \bar\zeta^{1/2}\tilde p, \qquad \boldsymbol F = l_p\bar\zeta^{1/2}\tilde{\boldsymbol F}, \qquad \rho = \bar\rho\tilde\rho, \qquad K = \bar K\tilde K,$$
$$\gamma = \bar\zeta l_p^{-1}\tilde\gamma, \qquad L = l_p\tilde L, \qquad (z, \boldsymbol x) = l_p(\tilde z, \tilde{\boldsymbol x}), \qquad t = l_p\bar c^{-1}\tilde t$$

have the form (1), however, with the 'tilde' quantities. In this new frame the width of the random slab is of order one, the typical wavelength and the longitudinal correlation length are of order ε^2, and so on. From now on we drop the tildes.

In the dimensionless frame the source has the form

$$\boldsymbol F^\varepsilon(t, z, \boldsymbol x) = \frac{1}{\varepsilon} f\left(\frac{t}{\varepsilon^2}, \frac{\boldsymbol x}{\varepsilon}\right)\delta(z - L)\boldsymbol e_z, \tag{5}$$

where $f(t, \boldsymbol x)$ is the normalized source shape function (with time and spatial scales of variations of order one). The strong amplitude factor $1/\varepsilon$ ensures that the reflected wave has a typical amplitude of order one (this is in fact not important since the propagation

equations are linear). The Fourier transform in t of f is assumed to have a compact support contained in $\pm[\omega_0(1-B), \omega_0(1+B)]$, where ω_0 is the carrier frequency and $2B$ is the relative bandwidth.

The medium fluctuations have the form

$$\frac{1}{K^\varepsilon(z,\boldsymbol{x})} = \begin{cases} K_0^{-1}(z) & \text{if} \quad z \in (-\infty, 0), \\ K_0^{-1}(z)\left(1+\varepsilon\nu\left(z, \dfrac{z}{\varepsilon^2}, \dfrac{\boldsymbol{x}}{\varepsilon}\right)\right) & \text{if} \quad z \in (0, L), \\ K_0^{-1}(z) & \text{if} \quad z \in (L, \infty), \end{cases}$$

$$\rho^\varepsilon(z,\boldsymbol{x}) = \rho_0(z),$$

$$\gamma^\varepsilon(z,\boldsymbol{x}) = \begin{cases} 0 & \text{if} \quad z \in (-\infty, 0), \\ \gamma_0(z) & \text{if} \quad z \in (0, L), \\ 0 & \text{if} \quad z \in (L, \infty), \end{cases}$$

where K_0, ρ_0 and γ_0 are smooth functions (of class $\mathcal{C}^2$) with scales of variations of order one. The random field $\nu(z, z', \boldsymbol{x}')$ models the spatial fluctuations of the medium. For a fixed z, we assume that $(z', \boldsymbol{x}') \mapsto \nu(z, z', \boldsymbol{x}')$ is a zero-mean stationary random process which satisfies strong mixing conditions with respect to the variable z'. The dependence with respect to the first variable z models a variation along the longitudinal direction of the statistical properties of the random fluctuations. The important statistical information is contained in the autocorrelation function defined by

$$C(z, z', \boldsymbol{x}') = \mathbb{E}[\nu(z, z''+z', \boldsymbol{x}''+\boldsymbol{x}')\nu(z, z'', \boldsymbol{x}'')], \tag{6}$$

which is assumed to be at least twice differentiable at $\boldsymbol{x}' = \boldsymbol{0}$ and vanishing as $|\boldsymbol{x}'| \to \infty$.

Since both the medium and the source have transverse spatial variations at the scale ε, it is convenient to rescale the transverse variable $\boldsymbol{x}/\varepsilon \to \boldsymbol{x}$ and to introduce the rescaled fields $\boldsymbol{u}^\varepsilon$ and p^ε:

$$\boldsymbol{u}^\varepsilon(t, z, \boldsymbol{x}) = \boldsymbol{u}(t, z, \varepsilon\boldsymbol{x}), \qquad p^\varepsilon(t, z, \boldsymbol{x}) = p(t, z, \varepsilon\boldsymbol{x}). \tag{7}$$

The reader should keep in mind that thus, in the discussion below, when we refer to the transversal spatial parameter $\boldsymbol{x}$ it corresponds to $\varepsilon\boldsymbol{x}$ in the original coordinates.

2.2. Mode decomposition

In order to identify equations that give a convenient description of coupling between different wave modes we now decompose the pressure and longitudinal velocity fields as

$$p^\varepsilon(t, z, \boldsymbol{x}) = \frac{\zeta_0(z)^{1/2}}{2\pi} \int \left(\check{a}^\varepsilon(\omega, z, \boldsymbol{x})\, \mathrm{e}^{\mathrm{i}\frac{\omega\tau_0(z)}{\varepsilon^2}} + \check{b}^\varepsilon(\omega, z, \boldsymbol{x})\, \mathrm{e}^{-\mathrm{i}\frac{\omega\tau_0(z)}{\varepsilon^2}}\right) \mathrm{e}^{-\mathrm{i}\frac{\omega t}{\varepsilon^2}}\, \mathrm{d}\omega, \tag{8}$$

$$\boldsymbol{e}_z \cdot \boldsymbol{u}^\varepsilon(t, z, \boldsymbol{x}) = \frac{\zeta_0(z)^{-1/2}}{2\pi} \int \left(\check{a}^\varepsilon(\omega, z, \boldsymbol{x})\, \mathrm{e}^{\mathrm{i}\frac{\omega\tau_0(z)}{\varepsilon^2}} - \check{b}^\varepsilon(\omega, z, \boldsymbol{x})\, \mathrm{e}^{-\mathrm{i}\frac{\omega\tau_0(z)}{\varepsilon^2}}\right) \mathrm{e}^{-\mathrm{i}\frac{\omega t}{\varepsilon^2}}\, \mathrm{d}\omega, \tag{9}$$

where $\check{a}^\varepsilon$ and $\check{b}^\varepsilon$ are right-propagating and left-propagating modes, respectively. Here we have introduced the background impedance $\zeta_0(z)$, velocity $c_0(z)$ and travel time $\tau_0(z)$:

$$\zeta_0(z) = \sqrt{K_0(z)\rho_0(z)}, \qquad c_0(z) = \frac{\sqrt{K_0(z)}}{\sqrt{\rho_0(z)}}, \qquad \tau_0(z) = \int_0^z \frac{\mathrm{d}z'}{c_0(z')}.$$

In the homogeneous medium ($\nu = 0$ and ρ_0, K_0, γ_0 independent of z), expressions (8) and (9) give a decomposition into uncoupled right- and left-propagating modes [6]. In the inhomogeneous case, by substituting (8) and (9) into the wave equations (1) we obtain the

Figure 1. Boundary conditions for the modes in the presence of a random slab $(0, L)$ and a source at $z = L$.

coupled mode equations:

$$\frac{\mathrm{d}\check{a}^\varepsilon}{\mathrm{d}z} = \mathcal{L}^\varepsilon \check{a}^\varepsilon + \mathrm{e}^{-2\mathrm{i}\frac{\omega\tau_0(z)}{\varepsilon^2}}\mathcal{L}^\varepsilon \check{b}^\varepsilon - \frac{\gamma_0(z)}{2\zeta_0(z)}\big(\check{a}^\varepsilon - \mathrm{e}^{-2\mathrm{i}\frac{\omega\tau_0(z)}{\varepsilon^2}}\check{b}^\varepsilon\big) - \frac{\zeta_0'(z)}{2\zeta_0(z)}\,\mathrm{e}^{-2\mathrm{i}\frac{\omega\tau_0(z)}{\varepsilon^2}}\check{b}^\varepsilon, \tag{10}$$

$$\frac{\mathrm{d}\check{b}^\varepsilon}{\mathrm{d}z} = -\mathrm{e}^{2\mathrm{i}\frac{\omega\tau_0(z)}{\varepsilon^2}}\mathcal{L}^\varepsilon \check{a}^\varepsilon - \mathcal{L}^\varepsilon \check{b}^\varepsilon - \frac{\gamma_0(z)}{2\zeta_0(z)}\big(\mathrm{e}^{2\mathrm{i}\frac{\omega\tau_0(z)}{\varepsilon^2}}\check{a}^\varepsilon - \check{b}^\varepsilon\big) - \frac{\zeta_0'(z)}{2\zeta_0(z)}\,\mathrm{e}^{2\mathrm{i}\frac{\omega\tau_0(z)}{\varepsilon^2}}\check{a}^\varepsilon, \tag{11}$$

where

$$\mathcal{L}^\varepsilon = \frac{\mathrm{i}\omega}{2c_0(z)\varepsilon}\nu\left(z, \frac{z}{\varepsilon^2}, \boldsymbol{x}\right) + \frac{\mathrm{i}}{2\frac{\omega}{c_0(z)} + 2\mathrm{i}\varepsilon^2\frac{\gamma_0(z)}{\zeta_0(z)}}\triangle_\perp,$$

$\triangle_\perp$ is the transverse Laplacian and ζ_0' is the spatial derivative of ζ_0. Note that the evolution equations (10) and (11) have terms with rapid phases and rapid random fluctuations. We anticipate that the terms with amplitudes of order one and rapid phases of the form $\exp(\pm 2\mathrm{i}\omega\tau_0(z)/\varepsilon^2)$ vanish in the limit $\varepsilon \to 0$ by homogenization arguments (however, the terms with rapid phases and large amplitudes of order ε^{-1} deserve particular attention). Note also that the random process appears in the scaled form $\frac{1}{\varepsilon}\nu\big(z, \frac{z}{\varepsilon^2}, \boldsymbol{x}\big)$, which is the scaling of the diffusion approximation regime, thus we anticipate that these terms will give rise to Brownian fields in the limit $\varepsilon \to 0$.

Finally, we remark that indeed the right- and left-propagating modes give a complete description with the transverse velocity field $\boldsymbol{e}_{x_i} \cdot \boldsymbol{u}^\varepsilon(t, z, \boldsymbol{x})$, $i = 1, \ldots, d$, deriving from the modes $\check{a}^\varepsilon$ and $\check{b}^\varepsilon$ as

$$\boldsymbol{e}_{x_i} \cdot \boldsymbol{u}^\varepsilon(t, z, \boldsymbol{x}) = \frac{\zeta_0(z)^{-1/2}}{2\pi}\int \frac{-\varepsilon\mathrm{i}}{\frac{\omega}{c_0(z)} + \mathrm{i}\varepsilon^2\frac{\gamma_0(z)}{\zeta_0(z)}} \times \left(\frac{\partial\check{a}^\varepsilon}{\partial x_i}(\omega, z, \boldsymbol{x})\,\mathrm{e}^{\mathrm{i}\frac{\omega\tau_0(z)}{\varepsilon^2}} + \frac{\partial\check{b}^\varepsilon}{\partial x_i}(\omega, z, \boldsymbol{x})\,\mathrm{e}^{-\mathrm{i}\frac{\omega\tau_0(z)}{\varepsilon^2}}\right)\mathrm{e}^{-\mathrm{i}\frac{\omega t}{\varepsilon^2}}\,\mathrm{d}\omega.$$

2.3. Boundary conditions

The mode amplitudes $\check{a}^\varepsilon$ and $\check{b}^\varepsilon$ satisfy the system (10) and (11) in the random slab $z \in (0, L)$. This system is completed by boundary conditions corresponding to the presence of the source term (5) in the plane $z = L$ and the radiation condition at infinity, see figure 1.

Taking into account the fact that there is no source in $(-\infty, 0)$, the right-going mode amplitudes $\check{a}^\varepsilon$ are zero in this half-space. By the continuity of the fields p^ε and $\boldsymbol{e}_z \cdot \boldsymbol{u}^\varepsilon$ at $z = 0$, this gives the first boundary condition

$$\check{a}^\varepsilon(\omega, 0^+, \boldsymbol{x}) = 0, \qquad \check{b}^\varepsilon(\omega, 0^+, \boldsymbol{x}) = \check{b}^\varepsilon(\omega, 0^-, \boldsymbol{x}). \tag{12}$$

Taking into account the fact that there is no source in (L, ∞), the left-going mode amplitudes $\check{b}^\varepsilon$ are zero in this half-space. The jump conditions across the source interface

$z = L$ then give the relation

$$\check{b}^\varepsilon(\omega, L^-, \boldsymbol{x}) = \frac{1}{\varepsilon}\,\mathrm{e}^{\mathrm{i}\frac{\omega\tau_0(L)}{\varepsilon^2}}\check{b}_{\mathrm{s}}(\omega, \boldsymbol{x}), \qquad \check{b}_{\mathrm{s}}(\omega, \boldsymbol{x}) = -\frac{1}{2\zeta_0(L)^{1/2}}\check{f}(\omega, \boldsymbol{x}), \tag{13}$$

where the time Fourier transform is defined by

$$\check{f}(\omega, \boldsymbol{x}) = \int f(t, \boldsymbol{x})\,\mathrm{e}^{\mathrm{i}\omega t}\,\mathrm{d}t. \tag{14}$$

We also have

$$\check{a}^\varepsilon(\omega, L^+, \boldsymbol{x}) = \check{a}^\varepsilon(\omega, L^-, \boldsymbol{x}) - \frac{1}{\varepsilon}\,\mathrm{e}^{-\mathrm{i}\frac{\omega\tau_0(L)}{\varepsilon^2}}\check{b}_{\mathrm{s}}(\omega, \boldsymbol{x}),$$

which means that the field observed at L^+ is a right-going wave $\check{a}^\varepsilon(\omega, L^+, \boldsymbol{x})$ that is the superposition of the field reflected by the random slab, $\check{a}^\varepsilon(\omega, L^-, \boldsymbol{x})$, and of the field emitted to the right by the source. This direct source contribution is concentrated in time on a small interval with center at 0 and time width of order ε^2 and we will not take it into account in the following.

2.4. Reflection and transmission operators

The system (10) and (11) is complemented by the boundary conditions (12) and (13) at $z = 0$ and $z = L$. As a consequence, the modes $(\check{a}^\varepsilon, \check{b}^\varepsilon)$ are not adapted to the filtration of the random process ν, so that the limit theorems for the solutions of random differential equations cannot be applied directly, but a preliminary invariant imbedding step is necessary to obtain adapted processes. We introduce reflection and transmission operators by defining the transverse Fourier modes by

$$\hat{a}^\varepsilon(\omega, z, \boldsymbol{\kappa}) = \int \check{a}^\varepsilon(\omega, z, \boldsymbol{x})\,\mathrm{e}^{-\mathrm{i}\boldsymbol{\kappa}\cdot\boldsymbol{x}}\,\mathrm{d}\boldsymbol{x}, \qquad \hat{b}^\varepsilon(\omega, z, \boldsymbol{\kappa}) = \int \check{b}^\varepsilon(\omega, z, \boldsymbol{x})\,\mathrm{e}^{-\mathrm{i}\boldsymbol{\kappa}\cdot\boldsymbol{x}}\,\mathrm{d}\boldsymbol{x}, \tag{15}$$

and by making the ansatz for $z \in (0, L)$:

$$\hat{b}^\varepsilon(\omega, 0, \boldsymbol{\kappa}) = \int \hat{T}^\varepsilon(\omega, z, \boldsymbol{\kappa}, \boldsymbol{\kappa}')\hat{b}^\varepsilon(\omega, z, \boldsymbol{\kappa}')\,\mathrm{d}\boldsymbol{\kappa}', \tag{16}$$

$$\hat{a}^\varepsilon(\omega, z, \boldsymbol{\kappa}) = \int \hat{\mathcal{R}}^\varepsilon(\omega, z, \boldsymbol{\kappa}, \boldsymbol{\kappa}')\hat{b}^\varepsilon(\omega, z, \boldsymbol{\kappa}')\,\mathrm{d}\boldsymbol{\kappa}'. \tag{17}$$

The incoming wave is given by $\hat{b}^\varepsilon(\omega, L^-, \boldsymbol{\kappa}')$, the operator $\hat{T}^\varepsilon(\omega, L, \boldsymbol{\kappa}, \boldsymbol{\kappa}')$ maps it to the wave $\hat{b}^\varepsilon(\omega, 0, \boldsymbol{\kappa})$ transmitted to $z = 0$ while the operator $\hat{\mathcal{R}}^\varepsilon(\omega, L, \boldsymbol{\kappa}, \boldsymbol{\kappa}')$ maps it to the wave $\hat{a}^\varepsilon(\omega, L^-, \boldsymbol{\kappa})$ reflected from the random slab at $z = L$.

Using the mode coupling equations (10) and (11) one finds

$$\begin{aligned}
\frac{\mathrm{d}}{\mathrm{d}z}\hat{\mathcal{R}}^\varepsilon(\omega, z, \boldsymbol{\kappa}, \boldsymbol{\kappa}') &= -\frac{\gamma_0(z)}{\zeta_0(z)}\hat{\mathcal{R}}^\varepsilon(\omega, z, \boldsymbol{\kappa}, \boldsymbol{\kappa}') + \mathrm{e}^{-2\mathrm{i}\frac{\omega\tau_0(z)}{\varepsilon^2}}\hat{\mathcal{L}}^\varepsilon(\omega, z, \boldsymbol{\kappa}, \boldsymbol{\kappa}') \\
&\quad + \mathrm{e}^{2\mathrm{i}\frac{\omega\tau_0(z)}{\varepsilon^2}}\iint \hat{\mathcal{R}}^\varepsilon(\omega, z, \boldsymbol{\kappa}, \boldsymbol{\kappa}_1)\hat{\mathcal{L}}^\varepsilon(\omega, z, \boldsymbol{\kappa}_1, \boldsymbol{\kappa}_2)\hat{\mathcal{R}}^\varepsilon(\omega, z, \boldsymbol{\kappa}_2, \boldsymbol{\kappa}')\,\mathrm{d}\boldsymbol{\kappa}_1\,\mathrm{d}\boldsymbol{\kappa}_2 \\
&\quad + \int \hat{\mathcal{L}}^\varepsilon(\omega, z, \boldsymbol{\kappa}, \boldsymbol{\kappa}_1)\hat{\mathcal{R}}^\varepsilon(\omega, z, \boldsymbol{\kappa}_1, \boldsymbol{\kappa}') + \hat{\mathcal{R}}^\varepsilon(\omega, z, \boldsymbol{\kappa}, \boldsymbol{\kappa}_1)\hat{\mathcal{L}}^\varepsilon(\omega, z, \boldsymbol{\kappa}_1, \boldsymbol{\kappa}')\,\mathrm{d}\boldsymbol{\kappa}_1 \\
&\quad + \left(\frac{\gamma_0(z)}{2\zeta_0(z)} + \frac{\zeta_0'(z)}{2\zeta_0(z)}\right)\mathrm{e}^{2\mathrm{i}\frac{\omega\tau_0(z)}{\varepsilon^2}}\int \hat{\mathcal{R}}^\varepsilon(\omega, z, \boldsymbol{\kappa}, \boldsymbol{\kappa}_1)\hat{\mathcal{R}}^\varepsilon(\omega, z, \boldsymbol{\kappa}_1, \boldsymbol{\kappa}')\,\mathrm{d}\boldsymbol{\kappa}_1 \\
&\quad + \left(\frac{\gamma_0(z)}{\zeta_0(z)} + \frac{\zeta_0'(z)}{2\zeta_0(z)}\right)\mathrm{e}^{-2\mathrm{i}\frac{\omega\tau_0(z)}{\varepsilon^2}}\delta(\boldsymbol{\kappa} - \boldsymbol{\kappa}'),
\end{aligned} \tag{18}$$

$$\frac{\mathrm{d}}{\mathrm{d}z}\hat{\mathcal{T}}^{\varepsilon}(\omega,z,\boldsymbol{\kappa},\boldsymbol{\kappa}') = \frac{\gamma_0(z)}{2\zeta_0(z)}\hat{\mathcal{T}}^{\varepsilon}(\omega,z,\boldsymbol{\kappa},\boldsymbol{\kappa}') + \int \hat{\mathcal{T}}^{\varepsilon}(\omega,z,\boldsymbol{\kappa},\boldsymbol{\kappa}_1)\hat{\mathcal{L}}^{\varepsilon}(\omega,z,\boldsymbol{\kappa}_1,\boldsymbol{\kappa}')\,\mathrm{d}\boldsymbol{\kappa}_1$$
$$+\mathrm{e}^{2\mathrm{i}\frac{\omega\tau_0(z)}{\varepsilon^2}}\iint \hat{\mathcal{T}}^{\varepsilon}(\omega,z,\boldsymbol{\kappa},\boldsymbol{\kappa}_1)\hat{\mathcal{L}}^{\varepsilon}(\omega,z,\boldsymbol{\kappa}_1,\boldsymbol{\kappa}_2)\hat{\mathcal{R}}^{\varepsilon}(\omega,z,\boldsymbol{\kappa}_2,\boldsymbol{\kappa}')\,\mathrm{d}\boldsymbol{\kappa}_1\,\mathrm{d}\boldsymbol{\kappa}_2$$
$$+\left(\frac{\gamma_0(z)}{2\zeta_0(z)}+\frac{\zeta_0'(z)}{2\zeta_0(z)}\right)\mathrm{e}^{2\mathrm{i}\frac{\omega\tau_0(z)}{\varepsilon^2}}\int \hat{\mathcal{T}}^{\varepsilon}(\omega,z,\boldsymbol{\kappa},\boldsymbol{\kappa}_1)\hat{\mathcal{R}}^{\varepsilon}(\omega,z,\boldsymbol{\kappa}_1,\boldsymbol{\kappa}')\,\mathrm{d}\boldsymbol{\kappa}_1, \qquad (19)$$

where we have defined

$$\hat{\mathcal{L}}^{\varepsilon}(\omega,z,\boldsymbol{\kappa}_1,\boldsymbol{\kappa}_2) = \frac{\mathrm{i}\omega}{\varepsilon 2(2\pi)^d c_0(z)}\hat{\nu}\left(z,\frac{z}{\varepsilon^2},\boldsymbol{\kappa}_1-\boldsymbol{\kappa}_2\right) - \frac{\mathrm{i}|\boldsymbol{\kappa}_1|^2}{2\frac{\omega}{c_0(z)}+2\mathrm{i}\varepsilon^2\frac{\gamma_0(z)}{\zeta_0(z)}}\delta(\boldsymbol{\kappa}_1-\boldsymbol{\kappa}_2), \qquad (20)$$

with $\hat{\nu}(z,z',\boldsymbol{\kappa})$ the partial Fourier transform in $\boldsymbol{x}'$ of $\nu(z,z',\boldsymbol{x}')$ (as in (15)). This system is complemented with the initial conditions

$$\hat{\mathcal{R}}^{\varepsilon}(\omega,z=0,\boldsymbol{\kappa},\boldsymbol{\kappa}') = 0, \qquad \hat{\mathcal{T}}^{\varepsilon}(\omega,z=0,\boldsymbol{\kappa},\boldsymbol{\kappa}') = \delta(\boldsymbol{\kappa}-\boldsymbol{\kappa}'), \qquad (21)$$

corresponding to the boundary conditions (12) and (13). Note that the reflection and transmission operators are adapted to the filtration of the random process ν. The reflected wave field observed at the surface $z = L$ is

$$p^{\varepsilon}_{\mathrm{ref}}(t,\boldsymbol{x}) = \frac{\zeta_0(L)^{1/2}}{2\pi}\int \check{a}^{\varepsilon}(\omega,L^-,\boldsymbol{x})\,\mathrm{e}^{\mathrm{i}\frac{\omega\tau_0(L)}{\varepsilon^2}}\,\mathrm{e}^{-\mathrm{i}\frac{\omega t}{\varepsilon^2}}\,\mathrm{d}\omega$$
$$= \frac{\zeta_0(L)^{1/2}}{(2\pi)^{d+1}\varepsilon}\iiint \hat{\mathcal{R}}^{\varepsilon}(\omega,L,\boldsymbol{\kappa},\boldsymbol{\kappa}')\hat{b}_{\mathrm{s}}(\omega,\boldsymbol{\kappa}')\,\mathrm{e}^{\mathrm{i}\boldsymbol{\kappa}\cdot\boldsymbol{x}}\mathrm{e}^{\mathrm{i}\frac{\omega}{\varepsilon^2}[2\tau_0(L)-t]}\,\mathrm{d}\omega\,\mathrm{d}\boldsymbol{\kappa}\,\mathrm{d}\boldsymbol{\kappa}'.$$

It is thus clear that the statistical properties of the reflected field are determined by those of the reflection operator which in turn are determined by the medium parameters. We shall show how this fact can be exploited to infer knowledge about the medium based on observations of the reflected field.

Again the evolution equations (16) and (19) have terms with rapid phases and rapid random fluctuations and we anticipate that the terms with amplitudes of order one and rapid phases of the form $\exp(\pm 2\mathrm{i}\omega\tau_0(z)/\varepsilon^2)$ have only small impact on the quantities of interest in the limit $\varepsilon \to 0$. This is confirmed by our analysis in appendix A. Thus, the terms involving ζ_0' which reflect backscattering associated with variations in the homogenized medium have only a lower order influence. We stress that the inverse problem that we are considering here thus has a different character from the traditional context in which (strong) backscattering from the macroscale or homogenized medium is being used to for instance estimate velocity. We consider here a regime where the traditional approaches fail since coherent backscattering is relatively small and we have to use incoherent waves and their spectral contents for the task of inferring knowledge about the macroscale medium parameters. This approach was taken in [1], which dealt with the case of a perfectly layered medium, and the analysis here follows a similar vein.

3. Asymptotic analysis of the reflection operator

3.1. Transport equations in the weak backscattering regime

The analysis carried out in appendix A first shows that odd-order moments of the reflection operator are zero in the limit $\varepsilon \to 0$. As a result the mean reflected field is zero:

$$\lim_{\varepsilon\to 0}\mathbb{E}\big[p^{\varepsilon}_{\mathrm{ref}}(t,\boldsymbol{x})\big] = 0.$$

The cross correlations of the reflected wave field are not zero and they provide information about the medium. They can be written as

$$\lim_{\varepsilon\to 0}\mathbb{E}\big[p^{\varepsilon}_{\rm ref}(t,\boldsymbol{x})\,p^{\varepsilon}_{\rm ref}(t+\varepsilon^2 s,\boldsymbol{x}')\big]=\frac{\zeta_0(L)}{(2\pi)^{2d+1}}\int\cdots\int W_{(\boldsymbol{\kappa}_1,\boldsymbol{\kappa}_2),(\boldsymbol{\kappa}_3,\boldsymbol{\kappa}_4)}(\omega,t,L)$$
$$\times\,\mathrm{e}^{\mathrm{i}(\boldsymbol{\kappa}_1\cdot\boldsymbol{x}-\boldsymbol{\kappa}_3\cdot\boldsymbol{x}')}\mathrm{e}^{\mathrm{i}\omega s}\hat{b}_{\rm s}(\omega,\boldsymbol{\kappa}_2)\overline{\hat{b}_{\rm s}}(\omega,\boldsymbol{\kappa}_4)\,\mathrm{d}\omega\,\mathrm{d}\boldsymbol{\kappa}_1\,\mathrm{d}\boldsymbol{\kappa}_2\,\mathrm{d}\boldsymbol{\kappa}_3\,\mathrm{d}\boldsymbol{\kappa}_4, \tag{22}$$

where the cross spectral density W is defined by

$$W_{(\boldsymbol{\kappa}_1,\boldsymbol{\kappa}_2),(\boldsymbol{\kappa}_3,\boldsymbol{\kappa}_4)}(\omega,\tau,z)=\lim_{\varepsilon\to 0}\frac{1}{2\pi}\int\mathbb{E}\bigg[\hat{\mathcal{R}}^{\varepsilon}\Big(\omega+\frac{\varepsilon^2 h}{2},z,\boldsymbol{\kappa}_1,\boldsymbol{\kappa}_2\Big)$$
$$\times\,\overline{\hat{\mathcal{R}}^{\varepsilon}}\Big(\omega-\frac{\varepsilon^2 h}{2},z,\boldsymbol{\kappa}_3,\boldsymbol{\kappa}_4\Big)\bigg]\mathrm{e}^{-\mathrm{i}h[\tau-2\tau_0(z)]}\,\mathrm{d}h. \tag{23}$$

It is possible to give a complete description of the cross spectral density in the frequency band $[\omega_0-B,\omega_0+B]$ of the source and in the regime of *weak backscattering*. Weak backscattering occurs if

$$\delta:=\sup_{\boldsymbol{\kappa}\in\mathbb{R}^d,z\in(0,L),\omega\in[\omega_0(1-B),\omega_0(1+B)]}\frac{|\widehat{C}(z,2\omega/c_0(z),\boldsymbol{\kappa})|}{\widehat{C}(z,0,\mathbf{0})}\ll 1, \tag{24}$$

where $\widehat{C}$ is the Fourier transform of the autocorrelation function C defined by

$$\widehat{C}(z,k,\boldsymbol{\kappa})=\int_{\mathbb{R}^d}\int_{-\infty}^{\infty}C(z,z',\boldsymbol{x}')\,\mathrm{e}^{-\mathrm{i}(kz'+\boldsymbol{\kappa}\cdot\boldsymbol{x}')}\,\mathrm{d}z'\,\mathrm{d}\boldsymbol{x}'. \tag{25}$$

As can be seen in appendix A, the term $\widehat{C}(z,2\omega/c_0(z),\boldsymbol{\kappa})$ is proportional to the conversion rate (at location z) between right- and left-going modes, while $\widehat{C}(z,0,\boldsymbol{\kappa})$ is proportional to the conversion rate between two left-going modes (or between two right-going modes). In other words, δ is the ratio of the backscattering rate over the forward scattering rate.

Proposition 3.1. *In the weak backscattering regime the cross spectral density (23) has the form*

$$W_{(\boldsymbol{\kappa}_1,\boldsymbol{\kappa}_2),(\boldsymbol{\kappa}_3,\boldsymbol{\kappa}_4)}(\omega,\tau,z)=V_{\boldsymbol{\kappa}_2-\boldsymbol{\kappa}_4,\boldsymbol{\kappa}_1+\boldsymbol{\kappa}_4,\boldsymbol{\kappa}_1-\boldsymbol{\kappa}_2}(\omega,\tau,z)\delta(\boldsymbol{\kappa}_1-\boldsymbol{\kappa}_2-\boldsymbol{\kappa}_3+\boldsymbol{\kappa}_4), \tag{26}$$

where $V_{\boldsymbol{\kappa}_u,\boldsymbol{\kappa}_v,\boldsymbol{\kappa}_w}(\omega,\tau,z)$ is the solution of the system of transport equations

$$\frac{\partial V_{\boldsymbol{\kappa}_u,\boldsymbol{\kappa}_v,\boldsymbol{\kappa}_w}}{\partial z}+\frac{2}{c_0(z)}\frac{\partial V_{\boldsymbol{\kappa}_u,\boldsymbol{\kappa}_v,\boldsymbol{\kappa}_w}}{\partial\tau}=-\frac{2\gamma_0(z)}{\zeta_0(z)}V_{\boldsymbol{\kappa}_u,\boldsymbol{\kappa}_v,\boldsymbol{\kappa}_w}-\frac{\mathrm{i}c_0(z)}{\omega}\boldsymbol{\kappa}_u\cdot\boldsymbol{\kappa}_v V_{\boldsymbol{\kappa}_u,\boldsymbol{\kappa}_v,\boldsymbol{\kappa}_w}$$
$$+\frac{\omega^2}{4(2\pi)^d c_0^2(z)}\int\widehat{C}(z,0,\boldsymbol{\kappa})\{V_{\boldsymbol{\kappa}_u,\boldsymbol{\kappa}_v-\boldsymbol{\kappa},\boldsymbol{\kappa}_w-\boldsymbol{\kappa}}+V_{\boldsymbol{\kappa}_u,\boldsymbol{\kappa}_v-\boldsymbol{\kappa},\boldsymbol{\kappa}_w+\boldsymbol{\kappa}}+V_{\boldsymbol{\kappa}_u-\boldsymbol{\kappa},\boldsymbol{\kappa}_v,\boldsymbol{\kappa}_w-\boldsymbol{\kappa}}$$
$$+V_{\boldsymbol{\kappa}_u-\boldsymbol{\kappa},\boldsymbol{\kappa}_v,\boldsymbol{\kappa}_w+\boldsymbol{\kappa}}-V_{\boldsymbol{\kappa}_u-\boldsymbol{\kappa},\boldsymbol{\kappa}_v-\boldsymbol{\kappa},\boldsymbol{\kappa}_w}-V_{\boldsymbol{\kappa}_u+\boldsymbol{\kappa},\boldsymbol{\kappa}_v-\boldsymbol{\kappa},\boldsymbol{\kappa}_w}-2V_{\boldsymbol{\kappa}_u,\boldsymbol{\kappa}_v,\boldsymbol{\kappa}_w}\}\,\mathrm{d}\boldsymbol{\kappa}$$
$$+\frac{\omega^2}{4(2\pi)^d c_0^2(z)}\widehat{C}\Big(z,\frac{2\omega}{c_0(z)},\boldsymbol{\kappa}_w\Big)\delta(\tau), \tag{27}$$

starting from $V_{\boldsymbol{\kappa}_u,\boldsymbol{\kappa}_v,\boldsymbol{\kappa}_w}(\omega,\tau,z=0)=0$.

This proposition is proved in appendix A. It shows that the second-order statistics of the reflected wave depend on the macroscale features of the medium through the system of transport equations (27). The inverse (or imaging) problem consists in determining the coefficients of the transport equations from the solution V. In fact, we will see in the following that we do not need to know all of V in order to solve the inverse problem, because of the one-dimensional structure of the macroscale features of the medium.

3.2. Fraunhofer approximation and narrow bandwidth

It is possible to get closed-form expressions for physically relevant quantities from the system (27). These expressions become simple in a special regime that we now describe. We define the longitudinal (respectively transverse) correlation radius l_z (respectively l_x) of the random fluctuations and the standard deviation σ of the fluctuations as in (2)–(4). If we also introduce the typical speed of sound $\bar{c}$ of the medium, then the parameters

$$\alpha = \frac{\bar{c}L}{\omega_0 l_x^2}, \qquad \beta = \frac{\omega_0^2 L \sigma^2 l_z}{4\bar{c}^2}, \tag{28}$$

are the two dimensionless parameters that determine the behavior of the cross spectral density, as shown in appendix B. We remark that these parameters can either be computed using the original scaled parameters and C_K as in (2) or by using C in (6) along with non-dimensionalized parameters. The parameter α is the inverse of the Fresnel number that characterizes the strength of diffraction, while the parameter β characterizes the strength of random forward scattering. The strength of random backscattering relative to random forward scattering is δ defined by (24). In appendix D we analyze the behavior of the cross spectral density in the regime $\alpha \gg 1$ which corresponds to Fraunhofer approximation. The solution to the transport equations in this regime is given in lemmas D.1 and D.2. Under the additional assumption of narrow bandwidth $B \ll 1$ these results give in turn simple closed-form expressions for many physically relevant quantities and we discuss some of these in the following section. Accordingly we shall refer to the regime characterized by

$$\delta \ll 1, \qquad \alpha \gg 1, \qquad B \ll 1, \tag{29}$$

as the *Fraunhofer weak backscattering* regime.

4. The second-order statistics of the reflected waves

In this section we assume the weak backscattering regime described by assumption (24). In this regime we obtain an explicit expression for the intensity of the reflected wave in section 4.1. Under the additional assumption of Fraunhofer approximation and narrow bandwidth, that is, the Fraunhofer weak backscattering regime in (29), we obtain explicit expressions for the time-resolved reflected beam width, the spectral beam width, the spatial and spectral cross correlation functions in sections 4.2–4.5.

4.1. Mean reflected intensity

As a first application of proposition 3.1, we compute the mean reflected intensity at time t:

$$I^\varepsilon(t) = \frac{1}{\zeta_0(L)} \int \mathbb{E}\big[p^\varepsilon_{\rm ref}(t, \boldsymbol{x})^2\big]\, \mathrm{d}\boldsymbol{x}, \tag{30}$$

which is the total power reflected by the random slab at time t.

Proposition 4.1. *In the weak backscattering regime the mean reflected intensity $I^\varepsilon(t)$ has the limit $I(t)$ as $\varepsilon \to 0$:*

$$I(t) = \frac{1}{(2\pi)^{d+1}} \int P_{\rm ref}(\omega, t) \left[\int |\hat{b}_{\rm s}(\omega, \boldsymbol{\kappa}')|^2 \, \mathrm{d}\boldsymbol{\kappa}' \right] \mathrm{d}\omega, \tag{31}$$

where

$$P_{\rm ref}(\omega, t) = \frac{\omega^2}{8c_0(z(t))} \check{C}\left(z(t), \frac{2\omega}{c_0(z(t))}, \mathbf{0} \right) \exp\left(-2 \int_{z(t)}^{L} \frac{\gamma_0(z')}{\zeta_0(z')} \, \mathrm{d}z' \right). \tag{32}$$

Here $\check{C}$ is the partial Fourier transform of the autocorrelation function C

$$\check{C}(z,k,\boldsymbol{x}) = \int C(z,z',\boldsymbol{x})\,\mathrm{e}^{-\mathrm{i}kz'}\,\mathrm{d}z', \tag{33}$$

and we have assumed $z(t) \in (0,L)$ when defined such that

$$\int_{z(t)}^{L} \frac{1}{c_0(z')}\,\mathrm{d}z' = \frac{t}{2}. \tag{34}$$

This proposition is proved in appendix C. Remember that the total input energy is

$$E_{\mathrm{s}} = \frac{1}{(2\pi)^{d+1}} \int \left[\int |\hat{b}_{\mathrm{s}}(\omega,\boldsymbol{\kappa}')|^2\,\mathrm{d}\boldsymbol{\kappa}' \right] \mathrm{d}\omega, \tag{35}$$

so that $P_{\mathrm{ref}}(\omega,t)$ can be interpreted as the spectral density of power reflection at (or around) time t. We observe that the reflected intensity observed at time t corresponds to incoherent waves that have probed the medium from $z = L$ to $z = z(t)$ and that have been reflected at (or around) $z = z(t)$. In more detail:

(i) $P_{\mathrm{ref}}(\omega,t)$ and $I(t)$ are zero if $t \notin (0, 2\tau_0(L))$. The distance $z(t)$ corresponds to a round trip from L to $z(t)$ whose duration is t when moving with the background velocity $c_0(z)$.

(ii) The term $\frac{\omega^2}{8c_0(z(t))}\check{C}\big(z(t), \frac{2\omega}{c_0(z(t))}, \mathbf{0}\big)$ gives the generation rate of backpropagating wave energy at location $z(t)$ and frequency ω.

(iii) The term $\exp\big(-2\int_{z(t)}^{L} \frac{\gamma_0(z')}{\zeta_0(z')}\,\mathrm{d}z'\big)$ is the damping that occurs during a round trip from L to $z(t)$ in the absorbing medium.

If the background velocity c_0, impedance ζ_0, absorption γ_0 and the function $\check{C}$ do not depend on z, then the mean reflected intensity is zero if $t \notin (0, 2L/c_0)$. If $t \in (0, 2L/c_0)$, then we have $z(t) = L - c_0 t/2$ and

$$P_{\mathrm{ref}}(\omega,t) = \frac{\omega^2}{8c_0}\check{C}\left(\frac{2\omega}{c_0}, \mathbf{0}\right) \mathrm{e}^{-c_0 t \frac{\gamma_0}{\zeta_0}},$$

which shows that the reflected intensity decays exponentially in time due to absorption.

4.2. Beam width

We define the rms (root-mean-squared) width $R^{\varepsilon}(t)$ of the reflected wave at time t by

$$R^{\varepsilon 2}(t) = \frac{\int |\boldsymbol{x}|^2 \mathbb{E}\big[p^{\varepsilon}_{\mathrm{ref}}(t,\boldsymbol{x})^2\big]\,\mathrm{d}\boldsymbol{x}}{\int \mathbb{E}\big[p^{\varepsilon}_{\mathrm{ref}}(t,\boldsymbol{x})^2\big]\,\mathrm{d}\boldsymbol{x}}. \tag{36}$$

Proposition 4.2. *In the Fraunhofer weak backscattering regime (29) the beam width $R^{\varepsilon}(t)$ converges to $R(t)$ as $\varepsilon \to 0$, where $R(t)$ is given by*

$$\begin{aligned} R^2(t) = R_0^2 - \frac{1}{2}\int_{z(t)}^{L} c_0^{-2}(z')\Delta_{\boldsymbol{x}}\check{C}(z',0,\mathbf{0})[D_0(z(t))^2 + (D_0(z(t)) - D_0(z'))^2]\,\mathrm{d}z' \\ + 4\frac{K_0^2}{\omega_0^2} D_0(z(t))^2 + 4\frac{Q_0}{\omega_0} D_0(z(t)) - \frac{1}{\omega_0^2}\frac{\Delta_{\boldsymbol{x}}\check{C}\big(z(t), \frac{2\omega_0}{c_0(z(t))}, \mathbf{0}\big)}{\check{C}\big(z(t), \frac{2\omega_0}{c_0(z(t))}, \mathbf{0}\big)} D_0(z(t))^2. \end{aligned} \tag{37}$$

Here $z(t)$ is defined by (34), $D_0(z)$ is given by

$$D_0(z) = \int_{z}^{L} c_0(z')\,\mathrm{d}z', \tag{38}$$

R_0 (respectively K_0) is the rms beam width (respectively spectral width) of the input beam:

$$R_0^2 = \frac{\iint |\boldsymbol{x}|^2 |\check{b}_s(\omega, \boldsymbol{x})|^2 \, \mathrm{d}\boldsymbol{x} \, \mathrm{d}\omega}{\iint |\check{b}_s(\omega, \boldsymbol{x})|^2 \, \mathrm{d}\boldsymbol{x} \, \mathrm{d}\omega}, \qquad K_0^2 = \frac{\iint |\boldsymbol{\kappa}|^2 |\hat{b}_s(\omega, \boldsymbol{\kappa})|^2 \, \mathrm{d}\boldsymbol{\kappa} \, \mathrm{d}\omega}{\iint |\hat{b}_s(\omega, \boldsymbol{\kappa})|^2 \, \mathrm{d}\boldsymbol{\kappa} \, \mathrm{d}\omega}, \tag{39}$$

and Q_0 is defined by

$$Q_0 = \frac{\iint \boldsymbol{\kappa} \cdot \mathrm{Im}(\hat{b}_s \overline{\nabla_{\boldsymbol{\kappa}} \hat{b}_s}(\omega, \boldsymbol{\kappa})) \, \mathrm{d}\boldsymbol{\kappa} \, \mathrm{d}\omega}{\iint |\hat{b}_s(\omega, \boldsymbol{\kappa})|^2 \, \mathrm{d}\boldsymbol{\kappa} \, \mathrm{d}\omega} = \frac{-\iint \boldsymbol{x} \cdot \mathrm{Im}(\check{b}_s \overline{\nabla_{\boldsymbol{x}} \check{b}_s}(\omega, \boldsymbol{x})) \, \mathrm{d}\boldsymbol{x} \, \mathrm{d}\omega}{\iint |\check{b}_s(\omega, \boldsymbol{x})|^2 \, \mathrm{d}\boldsymbol{x} \, \mathrm{d}\omega}. \tag{40}$$

This proposition is proved in appendix E. For instance, in the case of a narrowband Gaussian beam $b_s(t, \boldsymbol{x})$ with a spatial chirp, obtained by sending a Gaussian beam with radius r_0 through a converging ($b_0 < 0$) or diverging ($b_0 > 0$) lens [10, section 18.4], we have

$$\hat{b}_s(\omega, \boldsymbol{\kappa}) = \hat{g}(\omega) \, \mathrm{e}^{-\frac{1}{2}(1+\mathrm{i}\frac{b_0}{\omega}) r_0^2 |\boldsymbol{\kappa}|^2}, \qquad R_0^2 = \frac{r_0^2}{2}\left(1 + \frac{b_0^2}{\omega_0^2}\right), \qquad K_0^2 = \frac{1}{2r_0^2}, \qquad Q_0 = \frac{b_0}{2\omega_0}, \tag{41}$$

with $\hat{g}$ being the Fourier transform of the pulse function of the source with carrier frequency ω_0.

We can interpret all terms in expression (37):

(i) The first term (with R_0) is the initial beam width.
(ii) The second term (with $\Delta_{\boldsymbol{x}} \check{C}(z', 0, \mathbf{0})$) is the spreading effect due to random forward scattering; it is the only term (along with the initial beam width) that is independent of ω_0 (i.e. of the frequency).
(iii) The third term (with K_0) is due to the natural beam diffraction.
(iv) The fourth term (with Q_0) is a convergence or divergence effect due to the curvature of the initial beam phase front; this term is the only one in the sum that can be negative; the condition $Q_0 < 0$ means that the input beam has an initial phase front that makes it converge, but this convergence is eventually overwhelmed by natural diffraction, and also by the spreading induced by random scattering.
(v) The last term (with $\Delta_{\boldsymbol{x}} \check{C}(z(t), \frac{2\omega_0}{c_0}, \mathbf{0})$) is the spreading induced by random backward scattering. This term is pointwise, in the sense that it depends only on the properties of the medium at $z(t)$, while the forward scattering term (ii) is cumulative and depends on the properties of the medium between $z(t)$ and L.

If the background velocity c_0 and the function $\check{C}$ do not depend on z, then the squared rms radius has a cubic polynomial expression in terms of $t \in (0, 2L/c_0)$:

$$R^2(t) = R_0^2 - \frac{2}{3}\Delta_{\boldsymbol{x}} \check{C}(0, \mathbf{0}) \left(\frac{c_0 t}{2}\right)^3 + 4\frac{K_0^2 c_0^2}{\omega_0^2}\left(\frac{c_0 t}{2}\right)^2 + 4\frac{Q_0 c_0}{\omega_0}\left(\frac{c_0 t}{2}\right) - \frac{c_0^2}{\omega_0^2}\frac{\Delta_{\boldsymbol{x}} \check{C}\left(\frac{2\omega_0}{c_0}, \mathbf{0}\right)}{\check{C}\left(\frac{2\omega_0}{c_0}, \mathbf{0}\right)}\left(\frac{c_0 t}{2}\right)^2. \tag{42}$$

This shows that random forward scattering is the dominant phenomenon for long times and that the beam width increases like $t^{3/2}$. The increase rate $t^{3/2}$ of the beam width is specific to our regime in which the medium fluctuations are anisotropic (the longitudinal correlation length is much smaller than the transverse correlation length). The increase rate of the beam width in an isotropic random medium is known to be $t^{1/2}$ and can be obtained by the radiative transfer or diffusion theory [12].

4.3. Spectral width

We define the rms spectral width $K^\varepsilon(t)$ of the reflected wave at time t by

$$K^{\varepsilon\,2}(t) = \frac{\int \mathbb{E}\big[\big|\nabla_{\boldsymbol{x}} p^\varepsilon_{\rm ref}(t,\boldsymbol{x})\big|^2\big]\,\mathrm{d}\boldsymbol{x}}{\int \mathbb{E}\big[p^\varepsilon_{\rm ref}(t,\boldsymbol{x})^2\big]\,\mathrm{d}\boldsymbol{x}} = \frac{\int |\boldsymbol{\kappa}|^2 \mathbb{E}\big[\big|\hat{p}^\varepsilon_{\rm ref}(t,\boldsymbol{\kappa})\big|^2\big]\,\mathrm{d}\boldsymbol{\kappa}}{\int \mathbb{E}\big[\big|\hat{p}^\varepsilon_{\rm ref}(t,\boldsymbol{\kappa})\big|^2\big]\,\mathrm{d}\boldsymbol{\kappa}}. \tag{43}$$

Proposition 4.3. *In the Fraunhofer weak backscattering regime the spectral width $K^\varepsilon(t)$ converges to $K(t)$ as $\varepsilon \to 0$, where $K(t)$ is given by*

$$K^2(t) = K_0^2 - \frac{\omega_0^2}{2}\int_{z(t)}^{L} c_0^{-2}(z')\Delta_{\boldsymbol{x}}\check{C}(z',0,\mathbf{0})\,\mathrm{d}z' - \frac{\Delta_{\boldsymbol{x}}\check{C}\big(z(t),\frac{2\omega_0}{c_0(z(t))},\mathbf{0}\big)}{\check{C}\big(z(t),\frac{2\omega_0}{c_0(z(t))},\mathbf{0}\big)}. \tag{44}$$

This proposition is proved in appendix F. In expression (44),

(i) The first term K_0^2 is the initial spectral width (squared).
(ii) The second term (with $\Delta_{\boldsymbol{x}}\check{C}(z',0,\mathbf{0})$) is the spectral broadening due to random forward scattering during the round trip from L to $z(t)$.
(iii) The third term is the spectral broadening due to random backward scattering at $z(t)$.

If the background velocity c_0 and the function $\check{C}$ do not depend on z, then the squared rms spectral width is a linear expression in terms of $t \in (0, 2L/c_0)$:

$$K^2(t) = K_0^2 - \frac{\omega_0^2}{2c_0^2}\Delta_{\boldsymbol{x}}\check{C}(0,\mathbf{0})\left(\frac{c_0 t}{2}\right) - \frac{\Delta_{\boldsymbol{x}}\check{C}\big(\frac{2\omega_0}{c_0},\mathbf{0}\big)}{\check{C}\big(\frac{2\omega_0}{c_0},\mathbf{0}\big)}. \tag{45}$$

This shows that the spectral broadening is dominated by random forward scattering for long times and that the spectral width grows like $t^{1/2}$.

4.4. Spatial cross correlation function

Here we consider the spatial cross correlation function:

$$A^\varepsilon(t,\boldsymbol{x}) = \frac{\int \mathbb{E}\big[p^\varepsilon_{\rm ref}(t,\boldsymbol{x}')\,p^\varepsilon_{\rm ref}(t,\boldsymbol{x}'+\boldsymbol{x})\big]\,\mathrm{d}\boldsymbol{x}'}{\int \mathbb{E}\big[p^\varepsilon_{\rm ref}(t,\boldsymbol{x}')^2\big]\,\mathrm{d}\boldsymbol{x}'}.$$

Proposition 4.4. *In the Fraunhofer weak backscattering regime the spatial cross correlation function $A^\varepsilon(t,\boldsymbol{x})$ has the limit $A(t,\boldsymbol{x})$ as $\varepsilon \to 0$, where $A(t,\boldsymbol{x})$ is given by*

$$A(t,\boldsymbol{x}) = A_0(\boldsymbol{x})\frac{\check{C}\big(z(t),\frac{2\omega_0}{c_0(z(t))},\boldsymbol{x}\big)}{\check{C}\big(z(t),\frac{2\omega_0}{c_0(z(t))},\mathbf{0}\big)}\exp\left(\frac{\omega_0^2}{2}\int_{z(t)}^{L} c_0^{-2}(z')[\check{C}(z',0,\boldsymbol{x}) - \check{C}(z',0,\mathbf{0})]\,\mathrm{d}z'\right), \tag{46}$$

$$A_0(\boldsymbol{x}) = \frac{\iint \mathrm{e}^{-\mathrm{i}\boldsymbol{\kappa}'\cdot\boldsymbol{x}}|\hat{b}_{\rm s}(\omega,\boldsymbol{\kappa}')|^2\,\mathrm{d}\boldsymbol{\kappa}'\,\mathrm{d}\omega}{\iint |\hat{b}_{\rm s}(\omega,\boldsymbol{\kappa}')|^2\,\mathrm{d}\boldsymbol{\kappa}'\,\mathrm{d}\omega}. \tag{47}$$

This proposition is proved in appendix G. There are three factors in the spatial cross correlation function (46):

(i) The first factor $A_0(\boldsymbol{x})$ is the contribution of the spatial diversity of the input beam.
(ii) The second factor gives the spatial decorrelation that is associated with the random backscattering at $z(t)$.

(iii) The third factor is the decorrelation deriving from the random forward scattering during the round trip from L to $z(t)$ and back.

If the background velocity c_0 and the function $\check{C}$ do not depend on z, then we have for any $t \in (0, 2L/c_0)$:

$$A(t, \boldsymbol{x}) = A_0(\boldsymbol{x}) \frac{\check{C}\left(\frac{2\omega_0}{c_0}, \boldsymbol{x}\right)}{\check{C}\left(\frac{2\omega_0}{c_0}, \mathbf{0}\right)} \exp\left(\frac{\omega_0^2}{2c_0^2}[\check{C}(0, \boldsymbol{x}) - \check{C}(0, \mathbf{0})]\left(\frac{c_0 t}{2}\right)\right).$$

This shows that, for small times, the cross correlation function is determined by the form of the input beam and the spatial distribution of the backscattering process. For times large enough so that $\beta(c_0 t)/L \gg 1$, the cross correlation function is determined by random forward scattering and we have approximately, if $\check{C}$ is isotropic in $\boldsymbol{x}$:

$$A(t, \boldsymbol{x}) \overset{\beta(c_0 t)/L \gg 1}{\simeq} A_0(\boldsymbol{x}) \frac{\check{C}\left(\frac{2\omega_0}{c_0}, \boldsymbol{x}\right)}{\check{C}\left(\frac{2\omega_0}{c_0}, \mathbf{0}\right)} \exp\left(\frac{\omega_0^2 t}{4c_0 d} \Delta_{\boldsymbol{x}} \check{C}(0, \mathbf{0}) |\boldsymbol{x}|^2\right),$$

which shows that the correlation radius decays as $t^{-1/2}$.

4.5. Spectral cross correlation function

Here we consider the spectral cross correlation function:

$$S^\varepsilon(t, \boldsymbol{\kappa}) = \frac{\int \mathbb{E}\left[\hat{p}^\varepsilon_{\mathrm{ref}}(t, \boldsymbol{\kappa}') \overline{\hat{p}^\varepsilon_{\mathrm{ref}}}(t, \boldsymbol{\kappa}' + \boldsymbol{\kappa})\right] \mathrm{d}\boldsymbol{\kappa}'}{\int \mathbb{E}\left[\left|\hat{p}^\varepsilon_{\mathrm{ref}}(t, \boldsymbol{\kappa}')\right|^2\right] \mathrm{d}\boldsymbol{\kappa}'}.$$

Proposition 4.5. *In the Fraunhofer weak backscattering regime the spectral cross correlation function $S^\varepsilon(t, \boldsymbol{\kappa})$ has the limit $S(t, \boldsymbol{\kappa})$ as $\varepsilon \to 0$, where $S(t, \boldsymbol{\kappa})$ is given by*

$$\begin{aligned} S(t, \boldsymbol{\kappa}) = {} & A_0\left(2\frac{D_0(z(t))}{\omega_0}\boldsymbol{\kappa}\right) \frac{\check{C}\left(z(t), \frac{2\omega_0}{c_0(z(t))}, \frac{D_0(z(t))}{\omega_0}\boldsymbol{\kappa}\right)}{\check{C}\left(z(t), \frac{2\omega_0}{c_0(z(t))}, \mathbf{0}\right)} \\ & \times \exp\left(\frac{\omega_0^2}{4}\int_{z(t)}^L c_0^{-2}(z') \left\{\check{C}\left(z', 0, [2D_0(z(t)) - D_0(z')]\frac{\boldsymbol{\kappa}}{\omega_0}\right)\right.\right. \\ & \left.\left. + \check{C}\left(z', 0, D_0(z')\frac{\boldsymbol{\kappa}}{\omega_0}\right) - 2\check{C}(z', 0, \mathbf{0})\right\} \mathrm{d}z'\right). \end{aligned} \tag{48}$$

This proposition is proved in appendix H. If the background velocity c_0 and the function $\check{C}$ do not depend on z, then we have for any $t \in (0, 2L/c_0)$:

$$S(t, \boldsymbol{\kappa}) = A_0\left(c_0 t \frac{c_0\boldsymbol{\kappa}}{\omega_0}\right) \frac{\check{C}\left(\frac{2\omega_0}{c_0}, \frac{c_0 t}{2}\frac{c_0\boldsymbol{\kappa}}{\omega_0}\right)}{\check{C}\left(\frac{2\omega_0}{c_0}, \mathbf{0}\right)} \exp\left(\frac{\omega_0^2}{4c_0^2}\int_0^{c_0 t} \left\{\check{C}\left(0, z'\frac{c_0\boldsymbol{\kappa}}{\omega_0}\right) - \check{C}(0, \mathbf{0})\right\} \mathrm{d}z'\right).$$

If $\beta \ll 1$ (i.e. if random forward scattering is weak), then the form of the spectral cross correlation function is determined by the input beam and the backscattering process. If $\beta \gg 1$, then the cross correlation function is determined by random forward scattering and we have approximately, if $\check{C}$ is isotropic in $\boldsymbol{x}$:

$$S(t, \boldsymbol{\kappa}) \overset{\beta \gg 1}{\simeq} A_0\left(c_0 t \frac{c_0\boldsymbol{\kappa}}{\omega_0}\right) \frac{\check{C}\left(\frac{2\omega_0}{c_0}, \frac{c_0 t}{2}\frac{c_0\boldsymbol{\kappa}}{\omega_0}\right)}{\check{C}\left(\frac{2\omega_0}{c_0}, \mathbf{0}\right)} \exp\left(\frac{c_0^3 t^3}{24d} \Delta_{\boldsymbol{x}} \check{C}(0, \mathbf{0}) |\boldsymbol{\kappa}|^2\right),$$

which shows that the spectral coherence radius decays as $t^{-3/2}$.

5. Enhanced backscattering

In this section, we study the dynamics of enhanced backscattering, and compute the time-dependent maximum, angular width and shape of the enhanced backscattering cone. We consider the following experiment: for a given $\boldsymbol{\kappa}_0$, we send a quasi-plane wave with carrier frequency ω_0, carrier wave vector $\boldsymbol{\kappa}_0$, and angular aperture smaller than $\alpha^{-1}(\omega_0 l_x/\bar{c})^{-1}$. We record the reflected power in the backscattered direction $-\boldsymbol{\kappa}_0$ or close to it, in a cone of angular aperture of order $\alpha^{-1}(\omega_0 l_x/\bar{c})^{-1}$:

$$\begin{aligned}\left|\hat{p}^{\varepsilon}_{\rm ref}(t,-\boldsymbol{\kappa}_0+\boldsymbol{\kappa})\right|^2 &= \left|\int p^{\varepsilon}_{\rm ref}(t,\boldsymbol{x})\,{\rm e}^{-{\rm i}(-\boldsymbol{\kappa}_0+\boldsymbol{\kappa})\cdot\boldsymbol{x}}\,{\rm d}\boldsymbol{x}\right|^2\\ &= \frac{\zeta_0(L)}{(2\pi)^2\varepsilon}\left|\iint \hat{\mathcal{R}}^{\varepsilon}(\omega,L,-\boldsymbol{\kappa}_0+\boldsymbol{\kappa},\boldsymbol{\kappa}')\,{\rm e}^{{\rm i}\frac{\omega}{\varepsilon^2}[2\tau_0(L)-t]}\hat{b}_{\rm s}(\omega,\boldsymbol{\kappa}')\,{\rm d}\boldsymbol{\kappa}'\,{\rm d}\omega\right|^2.\end{aligned}$$

If we perform a series of such experiments with different incoming directions and average with respect to the incoming direction, then we observe, in the asymptotic regime $\varepsilon\to 0$,

$$P_{\boldsymbol{\kappa}}(t)=\lim_{\varepsilon\to 0}\frac{1}{(2\pi)^d\zeta_0(L)}\int \mathbb{E}\big[\big|\hat{p}^{\varepsilon}_{\rm ref}(t,-\boldsymbol{\kappa}_0+\boldsymbol{\kappa})\big|^2\big]\,{\rm d}\boldsymbol{\kappa}_0.$$

Proposition 5.1. *The mean reflected power observed in the relative direction $\boldsymbol{\kappa}$ (relatively to the backscattered direction) is*

$$\begin{aligned}P_{\boldsymbol{\kappa}}(t)=P_\infty(t)\Bigg[1-\exp\left(-\frac{\omega_0^2}{2}\int_{z(t)}^{L}c_0^{-2}(z')\check{C}(z',0,\mathbf{0})\,{\rm d}z'\right)\\ +\exp\left(\frac{\omega_0^2}{2}\int_{z(t)}^{L}c_0^{-2}(z')\left\{\check{C}\left(z',0,[D_0(L)-D_0(z')]\frac{\boldsymbol{\kappa}}{\omega_0}\right)-\check{C}(z',0,\mathbf{0})\right\}{\rm d}z'\right)\Bigg],\end{aligned}\tag{49}$$

in the Fraunhofer weak backscattering regime (29). Here $z(t)$ is defined by (34),

$$P_\infty(t)=\frac{\pi^d E_{\rm s}\omega_0^2}{8c_0(z(t))}\check{C}\left(z(t),\frac{2\omega_0}{c_0(z(t))},\mathbf{0}\right)\exp\left(-2\int_{z(t)}^{L}\frac{\gamma_0(z')}{\zeta_0(z')}\,{\rm d}z'\right),\tag{50}$$

and $E_{\rm s}$ is given by (35).

This proposition is proved in appendix I. The reflected power $P_{\boldsymbol{\kappa}}(t)$ goes from $P_\infty(t)$ for $\frac{\bar{c}L}{\omega_0 l_x}|\boldsymbol{\kappa}|\gg 1$ to the maximal value $P_\infty(t)\,f_{\rm EBC}(t)$ for $\boldsymbol{\kappa}=0$, where the enhancement factor is

$$f_{\rm EBC}(t)=2-\exp\left(-\frac{\omega_0^2}{2}\int_{z(t)}^{L}c_0^{-2}(z')\check{C}(z',0,\mathbf{0})\,{\rm d}z'\right).$$

If the background velocity c_0 and the function $\check{C}$ do not depend on z, then we have for any $t\in(0,2L/c_0)$:

$$P_{\boldsymbol{\kappa}}(t)=P_\infty(t)\left[1-{\rm e}^{-\frac{\omega_0^2}{4c_0}\check{C}(0,\mathbf{0})t}+\exp\left(\frac{\omega_0^2}{2c_0^2}\int_0^{c_0t/2}\left\{\check{C}\left(0,c_0z'\frac{\boldsymbol{\kappa}}{\omega_0}\right)-\check{C}(0,\mathbf{0})\right\}{\rm d}z'\right)\right].$$

If random forward scattering is strong ($\beta\gg 1$) and $\check{C}$ is isotropic in $\boldsymbol{x}$, then for t large enough so that $\beta(c_0t/L)\gg 1$, we have

$$P_{\boldsymbol{\kappa}}(t)\simeq P_\infty(t)\left[1+\exp\left(\frac{c_0^3t^3}{96d}\Delta_{\boldsymbol{x}}\check{C}(0,\mathbf{0})|\boldsymbol{\kappa}|^2\right)\right],$$

which shows that the enhancement factor is 2 and the width of the cone decays as $t^{-3/2}$. Note that:

(i) The asymptotic Gaussian shape of the cone is obtained when the random fluctuations of the medium are smooth so that the autocorrelation function is twice differentiable at $\boldsymbol{x} = \mathbf{0}$. If the fluctuations are rough, then the cone has a cusp at $\boldsymbol{\kappa} = \mathbf{0}$ [8].

(ii) The decay rate $t^{-3/2}$ of the width of the cone is specific to our regime in which the medium fluctuations are anisotropic (the longitudinal correlation length is much smaller than the transverse correlation length). The decay rate of the width of the cone in an isotropic random medium is known to be $t^{-1/2}$ in the physical literature and can be obtained by diagrammatic expansions [17].

6. Statistical stability and inverse problems

6.1. Preliminary discussion

Here we discuss the conditions under which the second-order statistics of the reflected field can be observed. Formula (22) gives in particular

$$\lim_{\varepsilon\to 0}\frac{\int \mathbb{E}\big[p^\varepsilon_{\rm ref}(t,\boldsymbol{x})\,p^\varepsilon_{\rm ref}(t+\varepsilon^2 s,\boldsymbol{x})\big]\,\mathrm{d}\boldsymbol{x}}{\int \mathbb{E}\big[p^\varepsilon_{\rm ref}(t,\boldsymbol{x})^2\big]\,\mathrm{d}\boldsymbol{x}} = \frac{\int P_{\rm ref}(\omega,t)\,\mathrm{e}^{\mathrm{i}\omega s}\big[\int |\hat b_{\rm s}(\omega,\boldsymbol{\kappa}')|^2\,\mathrm{d}\boldsymbol{\kappa}'\big]\,\mathrm{d}\omega}{\int P_{\rm ref}(\omega,t)\big[\int |\hat b_{\rm s}(\omega,\boldsymbol{\kappa}')|^2\,\mathrm{d}\boldsymbol{\kappa}'\big]\,\mathrm{d}\omega},$$

which goes to zero when $s\to\infty$ by Riemann–Lebesgue lemma. This shows that the coherence time of the reflected wave is of order ε^2. Therefore, we can claim that, for any $p\in(0,2)$, we have

$$\lim_{\varepsilon\to 0}\frac{1}{2\varepsilon^p}\int_{t-\varepsilon^p}^{t+\varepsilon^p} p^\varepsilon_{\rm ref}(t',\boldsymbol{x})\,p^\varepsilon_{\rm ref}(t',\boldsymbol{x}')\,\mathrm{d}t' = \lim_{\varepsilon\to 0}\mathbb{E}\big[p^\varepsilon_{\rm ref}(t,\boldsymbol{x})\,p^\varepsilon_{\rm ref}(t,\boldsymbol{x}')\big].$$

A rigorous approach would make use of the fourth-order moments. This involves the study of $W_{p,q}$ for $n_p = n_q = 2$ (defined in appendix A), which is beyond the scope of this paper.

In the following section we discuss the problem of estimating the medium parameters. We again stress that we cannot expect, in our scaling regime, to estimate the actual pointwise parameters in (1). We can only estimate the homogenized medium or macroscale parameters that determine the reflected wave statistics. From proposition A.1 in appendix A it is clear that the medium parameters that determine the reflected wave statistics are

$$c_0(z),\qquad \frac{\gamma_0(z)}{\zeta_0(z)},\qquad C(z,z',\boldsymbol{x}). \tag{51}$$

Our objective is therefore to construct statistically stable functionals of the observations that give information about the macroscale parameters. We shall here focus on the Fraunhofer weak backscattering regime (29) in the case without absorption and when the data are the reflected intensity, beam and spectral width time profiles, respectively $I(t)$, $R(t)$ and $K(t)$, evaluated at particular source carriers and source chirp parameters: $\omega_{0,j}, b_{0,j}\, j = 1,2$. The power delay spread (i.e. the duration of the reflected wave) is of the order of $2L/\bar c$, while the coherence time is of the order of the initial pulse width ε^2. By time-windowing the reflected wave into time intervals long compared to the coherence time, but short compared to the power delay spread, one can get statistically stable estimates of the reflected intensity $I(t)$, the reflected beam width $R(t)$ and the spectral width $K(t)$. From these quantities, one can in particular reconstruct the background velocity $c_0(z)$ and the scattering coefficient $s(z)$:

$$s^2(z) = -\Delta_{\boldsymbol{x}}\check C(z,0,\mathbf{0}), \tag{52}$$

as we show in the following subsection.

6.2. Reconstruction of the background velocity and scattering coefficient

We discuss first the problem of estimating the background velocity. The identification of the background velocity is an important problem, in geophysics for instance [3]. As mentioned, in the cases with no strong interface that we consider, only the analysis of the incoherent reflected wave (as we carry out in this paper) can give an answer to this problem. We describe now how the background velocity can be extracted from the incoherent reflections by performing two experiments with two input Gaussian chirped beams of the form (41) with different chirps $b_{0,1}$ and $b_{0,2}$ (which affect R_0 and Q_0, but not K_0). We can then observe the differences between the reflected beam widths:

$$\delta_1(t) := \frac{\omega_0^2}{2}\frac{R^2(t,b_{0,2}) - R^2(t,b_{0,1}) - R_0^2(b_{0,2}) + R_0^2(b_{0,1})}{b_{0,2}-b_{0,1}} \overset{\text{in theory}}{=} \int_{z(t)}^{L} c_0(z')\,\mathrm{d}z'. \tag{53}$$

Using the fact that $\frac{\mathrm{d}z}{\mathrm{d}t} = -\frac{1}{2}c_0(z(t))$, we can compute $z(t)$ by integrating

$$\frac{\mathrm{d}z(t)}{\mathrm{d}t} = \sqrt{\frac{1}{2}}\sqrt{\frac{\mathrm{d}\delta_1(t)}{\mathrm{d}t}}, \qquad z(0) = L,$$

from which we can get the background velocity by the identity

$$c_0(z(t)) = \sqrt{2}\sqrt{\frac{\mathrm{d}\delta_1(t)}{\mathrm{d}t}}.$$

Alternatively, by performing two experiments with two input beams with zero chirp and with different carrier frequencies $\omega_{0,1}$ and $\omega_{0,2}$, we can extract from the reflected beam widths and spectral widths:

$$\tilde{\delta}_1(t) := \left[\frac{R^2(t,\omega_{0,2}) - R^2(t,\omega_{0,1})}{\frac{K^2(t,\omega_{0,2})+3K_0^2}{\omega_{0,2}^2} - \frac{K^2(t,\omega_{0,1})+3K_0^2}{\omega_{0,1}^2}}\right]^{1/2} \overset{\text{in theory}}{=} \int_{z(t)}^{L} c_0(z')\,\mathrm{d}z',$$

and we can use this result to extract the background velocity from $\tilde{\delta}_1(t)$ as described above for $\delta_1(t)$.

Beyond the background velocity, it is possible to extract the scattering coefficient by observing the spectral widths for two input beams with two different carrier frequencies $\omega_{0,1}$ and $\omega_{0,2}$:

$$\delta_2(t) := 2\frac{K^2(t,\omega_{0,2}) - K^2(t,\omega_{0,1})}{\omega_{0,2}^2 - \omega_{0,1}^2} \overset{\text{in theory}}{=} \int_{z(t)}^{L} c_0^{-2}(z')s^2(z')\,\mathrm{d}z'.$$

We can get the scattering coefficient $s^2(z)$ by the relation

$$s^2(z(t)) = 2\sqrt{2}\sqrt{\frac{\mathrm{d}\delta_1(t)}{\mathrm{d}t}}\frac{\mathrm{d}\delta_2(t)}{\mathrm{d}t}.$$

The results of this subsection show that the imaging problem can be solved, but they are difficult to implement in practice, because they require good estimates of derivatives of observable quantities, which are much less statistically stable than the observable quantities themselves. Practically, it is better to approximate the slowly varying parameters by stepwise constant functions, i.e. to assume that the medium is a stack of random layers which have constant background parameters. A least-square strategy can then be used to identify these parameters by fitting the observed quantities with the theoretical ones. A particular case is addressed in the following subsection.

6.3. Detection of an interface

In this subsection, we consider the situation in which the medium in $(0, L)$ is made of two materials. The slab $(L - z_i, L)$ close to the surface has constant background parameters c_0, ζ_0, γ_0 and stationary random fluctuations $\check{C}(z, k, \boldsymbol{x}) = \check{C}_0(k, \boldsymbol{x})$. The slab $(0, L - z_i)$ has constant background parameters c_1, ζ_1, γ_1 and stationary random fluctuations $\check{C}(z, k, \boldsymbol{x}) = \check{C}_1(k, \boldsymbol{x})$. By probing the medium with a beam and by observing the reflected wave, we aim to extract the parameters

$$c_j, \quad \gamma_j/\zeta_j, \quad s_j^2 = -\Delta\check{C}_j(0, \mathbf{0}), \qquad j = 0, 1, \quad z_i \text{ (interface location)}. \tag{54}$$

We first give the explicit expressions for the time-dependent reflected intensity, beam and spectral widths. The mean reflected intensity decays exponentially with time, but two exponential branches can be distinguished. More precisely,

$$I(t) = \begin{cases} \dfrac{\omega_0^2}{8c_0}\check{C}_0\left(\dfrac{2\omega_0}{c_0}, \mathbf{0}\right) \mathrm{e}^{-\frac{c_0\gamma_0}{\zeta_0}t} & \text{if} \quad t < t_i, \\ \dfrac{\omega_0^2}{8c_1}\check{C}_1\left(\dfrac{2\omega_0}{c_1}, \mathbf{0}\right) \mathrm{e}^{-\frac{c_0\gamma_0}{\zeta_0}t_i}\mathrm{e}^{-\frac{c_1\gamma_1}{\zeta_1}\tilde{t}} & \text{if} \quad t_i < t < t_i + 2\dfrac{L - z_i}{c_1}, \end{cases} \tag{55}$$

where $\tilde{t} = t - t_i$ and

$$t_i = 2\frac{z_i}{c_0}.$$

This shows that there is a jump in the mean reflected intensity at time t_i with the jump amplitude given by

$$\Delta I = \frac{\omega_0^2}{8}\left(\frac{1}{c_1}\check{C}_1\left(\frac{2\omega_0}{c_1}, \mathbf{0}\right) - \frac{1}{c_0}\check{C}_0\left(\frac{2\omega_0}{c_0}, \mathbf{0}\right)\right)\mathrm{e}^{-\frac{c_0\gamma_0}{\zeta_0}t_i}.$$

The spectral radius for $t < t_i$ is given by (45) and for $t_i < t < t_i + 2\frac{L-z_i}{c_1}$ by

$$K^2(t) = K_0^2 - \frac{\omega_0^2 t_i}{4c_0}\Delta_{\boldsymbol{x}}\check{C}_0(0, \mathbf{0}) - \frac{\omega_0^2\tilde{t}}{4c_1}\Delta_{\boldsymbol{x}}\check{C}_1(0, \mathbf{0}) - \frac{\Delta_{\boldsymbol{x}}\check{C}_1\left(\frac{2\omega_0}{c_1}, \mathbf{0}\right)}{\check{C}_1\left(\frac{2\omega_0}{c_1}, \mathbf{0}\right)},$$

where $\tilde{t} = t - t_i$. This shows that $K^2(t)$ is a piecewise-linear function, with a jump at time t_i whose amplitude is

$$\Delta K^2 = \frac{\Delta_{\boldsymbol{x}}\check{C}_0\left(\frac{2\omega_0}{c_0}, \mathbf{0}\right)}{\check{C}_0\left(\frac{2\omega_0}{c_0}, \mathbf{0}\right)} - \frac{\Delta_{\boldsymbol{x}}\check{C}_1\left(\frac{2\omega_0}{c_1}, \mathbf{0}\right)}{\check{C}_1\left(\frac{2\omega_0}{c_1}, \mathbf{0}\right)}.$$

The mean-squared radius $R^2(t)$ is a piecewise-cubic function. For $t < t_i$ is given by (42) and for $t_i < t < t_i + 2\frac{L-z_i}{c_1}$ by

$$\begin{aligned} R^2(t) = R_0^2 &- \Delta_{\boldsymbol{x}}\check{C}_0(0, \mathbf{0})\left(\frac{1}{8}\left(\frac{c_1^2\tilde{t}}{c_0}\right)^2(c_0t_i) + \frac{3}{16}\left(\frac{c_1^2\tilde{t}}{c_0}\right)(c_0t_i)^2 + \frac{1}{12}(c_0t_i)^3\right) \\ &- \Delta_{\boldsymbol{x}}\check{C}_1(0, \mathbf{0})\left(\frac{1}{12}(c_1\tilde{t})^3 + \frac{1}{8}\left(\frac{c_0^2t_i}{c_1}\right)(c_1\tilde{t})^2 + \frac{1}{16}\left(\frac{c_0^2t_i}{c_1}\right)^2(c_1\tilde{t})\right) \\ &+ \frac{K_0^2}{\omega_0^2}\left(c_1^2\tilde{t} + c_0^2t_i\right)^2 + 2\frac{Q_0}{\omega_0}\left(c_1^2\tilde{t} + c_0^2t_i\right) - \frac{1}{4\omega_0^2}\frac{\Delta_{\boldsymbol{x}}\check{C}_1\left(\frac{2\omega_0}{c_1}, \mathbf{0}\right)}{\check{C}_1\left(\frac{2\omega_0}{c_1}, \mathbf{0}\right)}\left(c_1^2\tilde{t} + c_0^2t_i\right)^2, \end{aligned} \tag{56}$$

where $\tilde{t} = t - t_i$. There is a jump of the beam radius at time t_i whose amplitude is

$$\Delta R^2 = \frac{c_0^4t_i^2}{4\omega_0^2}\left(\frac{\Delta_{\boldsymbol{x}}\check{C}_0\left(\frac{2\omega_0}{c_0}, \mathbf{0}\right)}{\check{C}_0\left(\frac{2\omega_0}{c_0}, \mathbf{0}\right)} - \frac{\Delta_{\boldsymbol{x}}\check{C}_1\left(\frac{2\omega_0}{c_1}, \mathbf{0}\right)}{\check{C}_1\left(\frac{2\omega_0}{c_1}, \mathbf{0}\right)}\right).$$

Therefore, by measuring the jump time t_i and the jump amplitudes ΔR^2 and ΔK^2 for the beam radius and spectral radius, we can extract the location of the interface and the background velocity c_0:

$$z_i = \sqrt[4]{\frac{\omega_0^2 t_i^2}{4}\frac{\Delta R^2}{\Delta K^2}}, \qquad c_0 = \frac{z_i}{t_i}.$$

From the slope of $t \mapsto K^2(t)$ and $t \mapsto \ln I(t)$ for $t < t_i$ we get the scattering coefficient s_0 and the absorption parameter γ_0/ζ_0:

$$s_0^2 = \frac{4c_0}{\omega_0^2}\frac{\mathrm{d}K^2(t)}{\mathrm{d}t}, \qquad \frac{\gamma_0}{\zeta_0} = -\frac{1}{c_0}\frac{\mathrm{d}\ln I(t)}{\mathrm{d}t}, \qquad \text{for} \quad 0 < t < t_i.$$

This completes the characterization of the parameters in the slab $(L - z_i, L)$. Next, from the slope of the logarithm of the reflected intensity for times $t > t_i$ we get $c_1\gamma_1/\zeta_1$:

$$\frac{c_1\gamma_1}{\zeta_1} = -\frac{\mathrm{d}\ln I(t)}{\mathrm{d}t}, \qquad \text{for} \quad t_i < t < t_i + 2\frac{L - z_i}{c_1}.$$

In order to get c_1, it is necessary to use two different input beams, either with two different chirps or with two different carrier frequencies. For instance, by performing two experiments with two input Gaussian chirped beams of the form (41) with different chirps $b_{0,1}$ and $b_{0,2}$, we can observe the differences between the reflected beam widths after time t_i:

$$\delta_1(t) = \frac{\omega_0^2}{2}\frac{R^2(t, b_{0,2}) - R^2(t, b_{0,1}) - R_0^2(b_{0,2}) + R_0^2(b_{0,1})}{b_{0,2} - b_{0,1}} \overset{\text{in theory}}{=} c_1^2\tilde{t} + c_0^2 t_i.$$

It is a linear function for $t_i < t < t_i + 2L - z_i/c_1$ whose slope is c_1^2. With c_1 and $c_1\gamma_1/\zeta_1$, we get the absorption coefficient γ_1/ζ_1. Finally, the slope of $K^2(t)$ after time t_i gives the scattering coefficient

$$s_1^2 = \frac{4c_1}{\omega_0^2}\frac{\mathrm{d}K^2(t)}{\mathrm{d}t}, \qquad \text{for} \quad t_i < t < t_i + 2\frac{L - z_i}{c_1}.$$

7. Numerical simulations

In this section we assume that there is no background impedance variation and no absorption, that is, $\zeta_0(z)$ is constant and $\gamma_0(z) \equiv 0$. We want in particular to extract the background velocity $c_0(z)$ from the measurements of the incoherent reflected waves. We also want to identify a sudden change in the statistics of the medium fluctuations. Observe that with no impedance contrast there will indeed be no strong interface in the medium generating a coherent reflected wave. The resolution of the full wave equation with several different scales is computationally expensive. Therefore the numerical simulations in a (1 + 1)-dimensional space are performed using the iterative scheme proposed in [9]. This scheme allows us to obtain the complex amplitudes $\check{a}(\omega, z, x)$ and $\check{b}(\omega, z, x)$ with a computational cost equivalent to the paraxial wave equation, but with comparable results to the full Helmholtz equation. The algorithm is as follows:

Step 0: start from $\check{a}_0(\omega, z, x) = 0$ for all z.

Step n: solve the paraxial wave equation with source from $z = L$ to $z = 0$:

$$\frac{\partial\check{b}_n}{\partial z} = -\frac{\mathrm{i}\omega}{2c_0(z)}\nu(z, x)\check{b}_n - \frac{\mathrm{i}c_0(z)}{2\omega}\triangle_\perp\check{b}_n - \mathrm{e}^{2\mathrm{i}\omega\tau_0(z)}\frac{\mathrm{i}\omega}{2c_0(z)}\nu(z, x)\check{a}_{n-1},$$

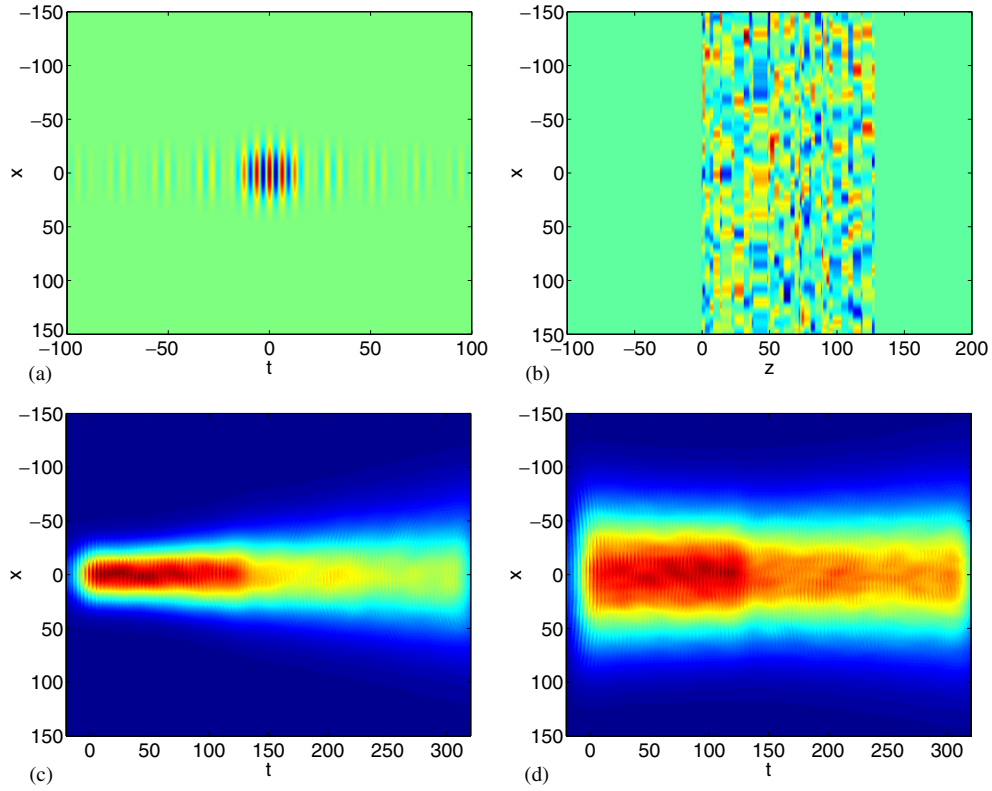

Figure 2. Picture (a): the source term $b_s(t, x)$ without chirp $b_{0,1} = 0$. Picture (b): one realization $\nu(z, x)$ of the random medium. Pictures (c) and (d): reflected intensities received with the unchirped incoming beam $b_{0,1} = 0$ (c) and with the chirped incoming beam $b_{0,2} = -2.5$ (d).

starting from $\check{b}_n(\omega, z = L, x) = \check{b}_s(\omega, x)$, and then solve the paraxial wave equation with source from $z = 0$ to $z = L$:

$$\frac{\partial \check{a}_n}{\partial z} = \frac{\mathrm{i}\omega}{2c_0(z)}\nu(z,x)\check{a}_n + \frac{\mathrm{i}c_0(z)}{2\omega}\triangle_\perp \check{a}_n + \mathrm{e}^{-2\mathrm{i}\omega\tau_0(z)}\frac{\mathrm{i}\omega}{2c_0(z)}\nu(z,x)\check{b}_n,$$

starting from $\check{a}_n(\omega, z = 0, x) = 0$. We use a split-step Fourier method for solving the random paraxial wave equations (while a finite-difference scheme was used in [9]). Although no convergence theory is (yet) available for this scheme, it has been shown to converge to the solution of the full wave equation by comparison with numerical simulations based on the Helmholtz equation. Moreover, we have observed that the scheme converges very quickly (after two or three steps) in the weak backscattering regime, even when random forward scattering is strong. This scheme is perfectly adapted to our setting.

7.1. Detection of background velocity change

In the first set of numerical simulations the medium consists of two different layers with the same statistics for the random fluctuations and different background velocities:

$$c_0(z) = \begin{cases} c_0 & \text{for} \quad z \in [L - z_i, L], \\ c_1 & \text{for} \quad z \in [0, L - z_i), \end{cases}$$

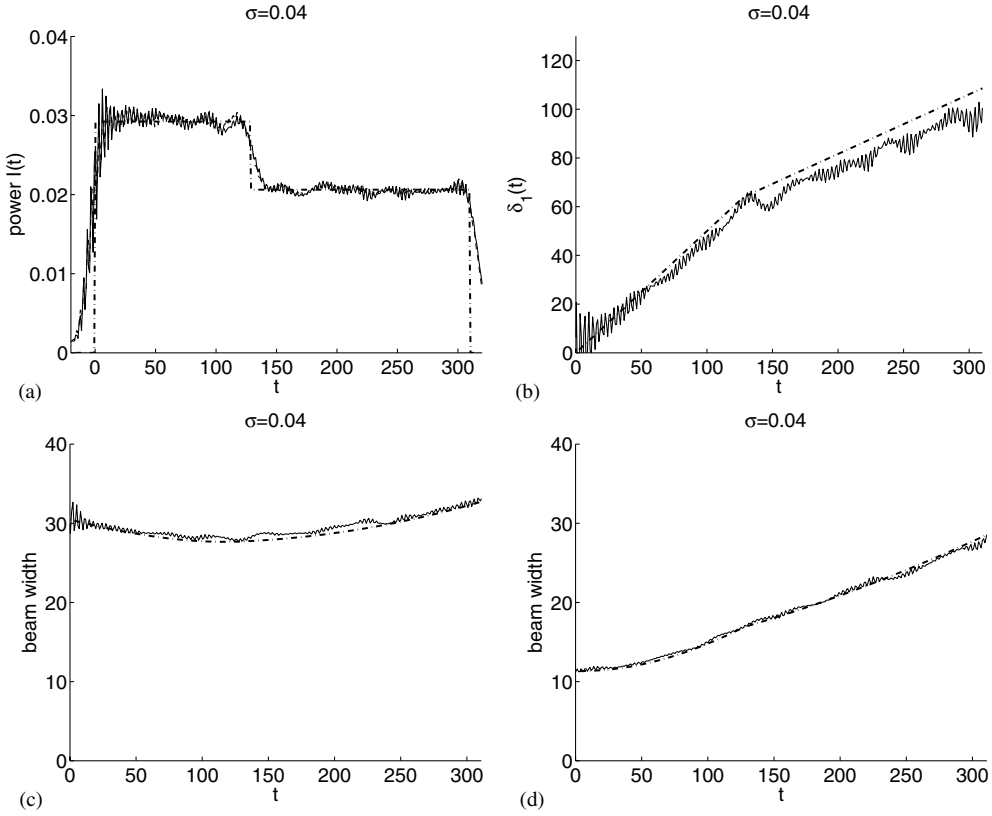

Figure 3. Picture (a): the mean reflected power $I(t)$ for the unchirped and chirped incoming beams (the two thin lines are almost undistinguishable). The thick dashed line is the theoretical value (55). Picture (b): the difference $\delta_1(t)$. The thin solid lines are the numerical results and the thick dashed line is the theoretical formula (58). Pictures (c) and (d): the rms reflected beam widths as a function of time for the unchirped incoming beam (c) and the chirped incoming beam (d). The thin solid lines are the numerical results and the thick dashed lines are the theoretical formulae (42) and (56).

with $L = 128$, $z_i = 64$, $c_0 = 1$ and $c_1 = 0.7$. The random process $\nu(z, x)$ has the form

$$\nu(z, x) = \sum_{j=0}^{\infty} \mathbf{1}_{[L_j, L_{j+1})}(z)\nu_j(x),$$

where $L_0 = 0$, $L_j = \sum_{i=1}^{j} l_i$; l_i are independent and identically distributed random variables with exponential distribution and mean $l_z = 4$; $\nu_j(x)$ are independent and identically distributed Gaussian processes with Gaussian autocorrelation function, standard deviation $\sigma = 0.04$, and transverse correlation length $l_x = 10$ (see figure 2(b)). We then have

$$\check{C}_{2k}(x) = \check{C}_0(0)\frac{1}{1 + 4k^2 l_z^2} \exp\left(-\frac{x^2}{l_x^2}\right), \qquad \check{C}_0(0) = 2\sigma^2 l_z.$$

The incoming beam has a Gaussian shape in space with radius $r_0 = 16$ and chirp b_0 (with $b_0 = 0$ or $b_0 = -2.5$) and a sinc shape in time with a central frequency $\omega_0 = 1$ (and central

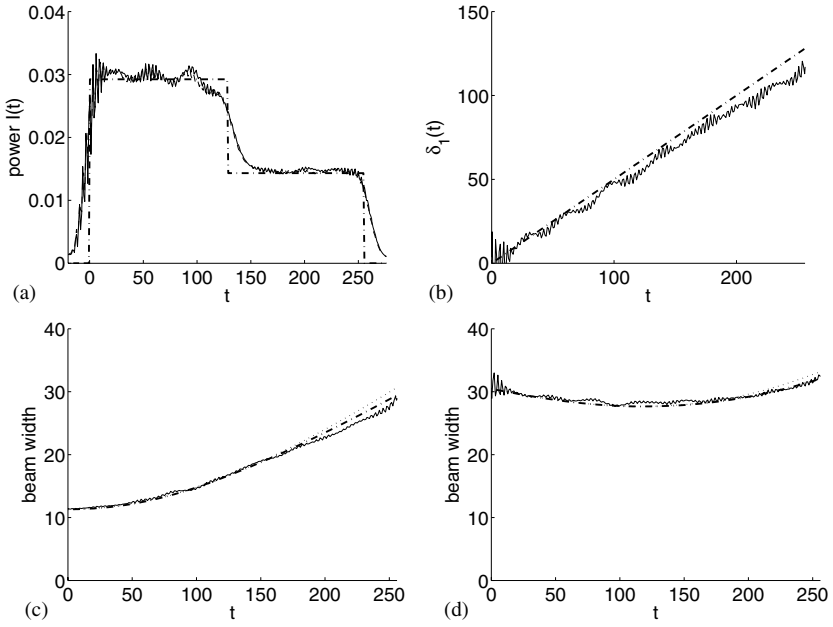

Figure 4. Characteristics of the reflected beam in the case of two heterogeneous layers with different standard deviations. Picture (a): the mean reflected power $I(t)$ for the unchirped and chirped incoming beams (the two thin lines are almost undistinguishable). The thick dashed line is the theoretical formula (55). Picture (b): the difference $\delta_1(t)$. The thin solid line is the numerical result and the thick dashed line stands the theoretical formula (58). Picture (c): the reflected beam radius for the unchirped beam. Picture (d): the reflected beam radius for the chirped beam. The thin solid lines are the numerical results and the thick dashed lines represent the theoretical formulae (42) and (56). The faint dotted lines are the theoretical radii if the standard deviation were 0.04 everywhere.

wave number $k_0 = 1$) and a bandwidth $B = 0.15$:

$$\hat{b}_s(\omega, \boldsymbol{\kappa}) = \mathbf{1}_{[\omega_0(1-B),\omega_0(1+B)]}(|\omega|) \exp\left(-\frac{1}{2}\left(1 + \mathrm{i}\frac{b_0}{\omega}\right) r_0^2 |\boldsymbol{\kappa}|^2\right). \tag{57}$$

Note that we have $\delta = \check{C}_{2k_0}(0)/\check{C}_0(0) \simeq 0.016$ which shows that we are indeed in the weak backscattering regime.

The separation of scales is not large in our numerical setup due to computational limitations. As a consequence:

(1) The spatial resolution of the inversion method (which is of the order of the pulse width times the background velocity) is not very high.

(2) The statistical stability property is not achieved and one needs to average over a series of independent experiments (here we average over 1000 experiments). In practice, this corresponds to repeating the experiments by moving the source to different (lateral) locations in order to probe different (quasi-independent) regions, while the one-dimensional background velocity profile is constant. This is feasible in a geophysical context. Note also that our theory predicts that this averaging should not be necessary when the separation of scales is large enough, although we cannot give a quantitative estimate.

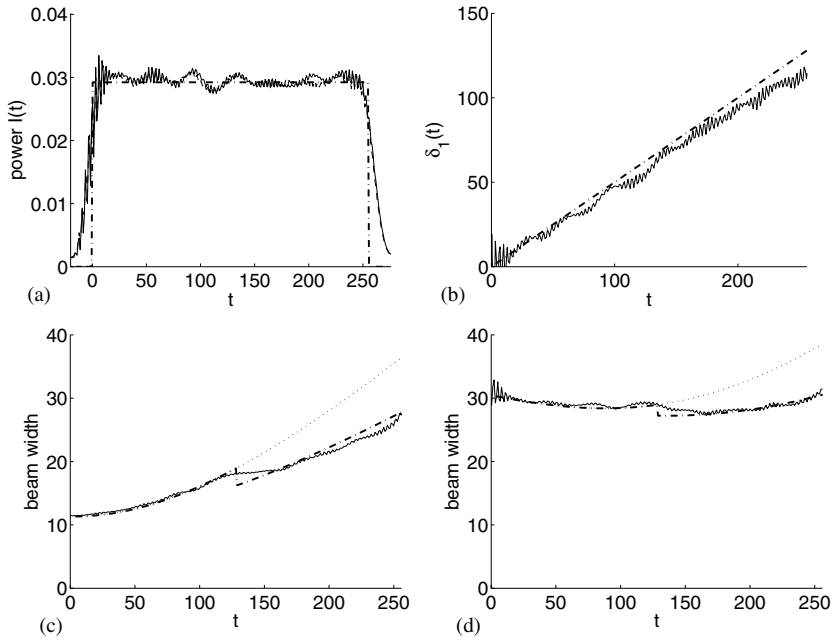

Figure 5. Characteristics of the reflected beam in the case of two heterogeneous layers with different transverse correlation radii. The subplots are defined as in figure 4. The faint dotted lines in pictures (c) and (d) are the theoretical radii if the correlation radii were $l_x = 8$ everywhere.

The medium is probed with two different incoming beams with two different chirp parameters $b_{0,1} = 0$ and $b_{0,2} = -2.5$ (the latter corresponding to a passage through a converging lens). The reflected signals are recorded (figures 2(c) and (d)), in particular the reflected powers $I(t, b_{0,1})$ and $I(t, b_{0,2})$ (figure 3(a)) and the reflected beam widths $R(t, b_{0,1})$ and $R(t, b_{0,2})$ (figures 3(c) and (d)). It can be checked that the reflected power does not depend on the chirp, while the reflected beam width depends on it. Difference (53) is the quantity that is used to determine the background velocity:

$$\delta_1^{(\mathrm{exp})}(t) = \frac{\omega_0^2}{2}\frac{R^2(t, b_{0,2}) - R^2(t, b_{0,1})}{b_{0,2} - b_{0,1}} - \frac{r_0^2}{4}(b_{0,2} + b_{0,1}),$$

and it is plotted in figure 3(b). By a least-square fit of the data $\delta_1^{(\mathrm{exp})}(t)$ with respect to the theoretical formula:

$$\delta_1^{(\mathrm{theo})}(t; c_0, c_1, z_i) = \begin{cases} \dfrac{c_0^2 t}{2} & \text{for} \quad t < t_i, \\ \dfrac{c_0^2 t_i}{2} + \dfrac{c_1^2(t - t_i)}{2} & \text{for} \quad t_i < t < T, \end{cases} \tag{58}$$

with $t_i = 2z_i/c_0$ and $T = 2z_i/c_0 + 2(L - z_i)/c_1$, we obtain the estimates $\hat{c_0} \simeq 0.97$, $\hat{c_1} \simeq 0.66$ and $\hat{z}_i \simeq 62$ for the quantities c_0, c_1 and z_i (the theoretical values are $c_0 = 1$, $c_1 = 0.7$ and $z_i = 64$).

7.2. Detection of change in microstructure

We next carry out a series of simulations with the same numerical model as in the previous subsection, however, we now examine the impact of two different types of background

variations: a jump in the standard deviation of the random fluctuations of the medium and a jump in the transverse correlation radius.

In figure 4, the background velocity $c_0 = 1$ and the transverse correlation length $l_x = 10$ are constant, but the standard deviation σ of the medium fluctuations goes from 0.04 in the region $[0, 64]$ to 0.028 in the region $[64, 128]$. The change in σ can be clearly seen in the jump of the reflected power. This jump is smooth because the separation of scales is not strong enough, and the pulse width is not much smaller than the total travel time. The resolution obtained with the use of the incoming beam (57) with the pulse shape $\mathrm{sinc}(Bt)$ is of the order of $2\pi c_0/B \sim 40$.

In figure 5, the background velocity $c_0 = 1$ and the standard deviation $\sigma = 0.04$ are constant, but the transverse correlation of the medium fluctuations goes from $l_x = 8$ in the region $[0, 64]$ to $l_x = 16$ in the region $[64, 128]$. In this case the reflected power is constant and the change in l_x can be seen in the jump of the mean radius.

8. Conclusions

We have presented a theoretical framework that in particular can be used to characterize the spectrum of waves reflected by a slab with anisotropic three-dimensional random fluctuations. We consider here the case when the reflected wave is weak and incoherent, corresponding to the absence of strong reflectors in the medium. We show how central quantities such as time-dependent wave intensity, beam width and spectral radius depend on the medium parameters through a system of transport equations.

Numerical simulations are carried out using a numerical scheme that is based on the analytic decomposition of the wave field introduced in the paper. The simulations demonstrate that information about the medium can be inferred from the spectrum of the reflections. In particular, we are able to detect a jump in the statistical properties of the medium fluctuations or in the background velocity by looking at the time dynamics of the reflected wave. The analytic framework we have presented is important for dealing with such an inverse problem where the useful information is contained in the wave spectrum.

The analysis proposed in this paper is tightly connected to the hypothesis that the background variations of the medium (that we want to image) are one dimensional. We do believe that an extension to three-dimensional background variations can be envisaged. We anticipate that the description of the wave spectrum should involve a system of transport equations along the characteristics of the slowly varying background. As long as caustics can be neglected, the analysis of the random backscattering and of the imaging problem should go along the same lines as those presented in this paper.

Acknowledgments

This work was supported by ONR grant N00014-02-1-0089 and DARPA grant N00014-05-1-0442. K Sølna was supported by NSF grant DMS0307011 and the Sloan Foundation.

Appendix A. The generalized system of transport equations

In this appendix we write the system of transport equations that determines the moments of the reflection operator. The next proposition generalizes the result obtained in [8] to the case in which the medium is absorbing and has slow variations of the background velocity and impedance. It shows that it is possible to compute the cross moments of the reflection operator using diffusion approximation theory in the white noise limit $\varepsilon \to 0$.

Proposition A.1. *Let us introduce some notations: if* $\boldsymbol{\kappa}_p(j), \boldsymbol{\kappa}'_p(j) \in \mathbb{R}^d$, $j = 1, \ldots, n_p$, *then the multi-vector* $\boldsymbol{p}$ *is the set*

$$\boldsymbol{p} = \{(\boldsymbol{\kappa}_p(j), \boldsymbol{\kappa}'_p(j))\}_{j=1}^{n_p}, \tag{A.1}$$

where $n_{\boldsymbol{p}}$ *stands for the number of pairs of* $\boldsymbol{p}$. *We introduce the high-order moments of products of* $\hat{\mathcal{R}}^\varepsilon(\omega, z, \boldsymbol{\kappa}, \boldsymbol{\kappa}')$, *the reflection process, at two nearby frequencies:*

$$\mathcal{U}^\varepsilon_{\boldsymbol{p},\boldsymbol{q}}(\omega, h, z) = \mathbb{E}\left[\prod_{j=1}^{n_p} \hat{\mathcal{R}}^\varepsilon\left(\omega + \frac{\varepsilon^2 h}{2}, z, \boldsymbol{\kappa}_p(j), \boldsymbol{\kappa}'_p(j)\right) \prod_{l=1}^{n_q} \overline{\hat{\mathcal{R}}^\varepsilon}\left(\omega - \frac{\varepsilon^2 h}{2}, z, \boldsymbol{\kappa}_q(l), \boldsymbol{\kappa}'_q(l)\right)\right], \tag{A.2}$$

where $\boldsymbol{p}, \boldsymbol{q}$ *are two multi-vectors of the form (A.1). We define the autocorrelation function of the fluctuations of the medium by (6) and its Fourier transform by (25) and*

$$\widehat{C}^\pm(z, k, \boldsymbol{\kappa}) = 2\int_{\mathbb{R}^d}\int_0^\infty C(z, z', \boldsymbol{x}')\, \mathrm{e}^{\pm \mathrm{i}kz' - \mathrm{i}\boldsymbol{\kappa}\cdot\boldsymbol{x}'}\, \mathrm{d}z'\, \mathrm{d}\boldsymbol{x}'. \tag{A.3}$$

The family of Fourier transforms

$$W^\varepsilon_{\boldsymbol{p},\boldsymbol{q}}(\omega, \tau, z) = \frac{1}{2\pi}\int \mathrm{e}^{-\mathrm{i}h[\tau - (n_{\boldsymbol{p}} + n_{\boldsymbol{q}})\tau_0(z)]} \mathcal{U}^\varepsilon_{\boldsymbol{p},\boldsymbol{q}}(\omega, h, z)\, \mathrm{d}h, \tag{A.4}$$

converges as $\varepsilon \to 0$ *to the solution* $W_{\boldsymbol{p},\boldsymbol{q}}$ *of the system of transport equations*

$$\frac{\partial W_{\boldsymbol{p},\boldsymbol{q}}}{\partial z} + \frac{n_{\boldsymbol{p}} + n_{\boldsymbol{q}}}{c_0(z)}\frac{\partial W_{\boldsymbol{p},\boldsymbol{q}}}{\partial \tau} = -\frac{\gamma_0(z)}{\zeta_0(z)}(n_{\boldsymbol{p}} + n_{\boldsymbol{q}})W_{\boldsymbol{p},\boldsymbol{q}} + \frac{\omega^2}{4(2\pi)^d c_0^2(z)}(\mathcal{L}_W W)_{\boldsymbol{p},\boldsymbol{q}} + \frac{\mathrm{i}c_0(z)}{2\omega}\left[\sum_{l=1}^{n_q}(|\boldsymbol{\kappa}_q(l)|^2 + |\boldsymbol{\kappa}'_q(l)|^2) - \sum_{j=1}^{n_p}(|\boldsymbol{\kappa}_p(j)|^2 + |\boldsymbol{\kappa}'_p(j)|^2)\right] W_{\boldsymbol{p},\boldsymbol{q}}, \tag{A.5}$$

with the initial conditions $W_{\boldsymbol{p},\boldsymbol{q}}(\omega, \tau, z = 0) = \mathbf{1}_0(n_{\boldsymbol{p}})\mathbf{1}_0(n_{\boldsymbol{q}})\delta(\tau)$. *Here the operator* $\mathcal{L}_W$ *is given by*

$$\begin{aligned}
(\mathcal{L}_W W)_{\boldsymbol{p},\boldsymbol{q}} = &-\int [n_{\boldsymbol{p}}\widehat{C}^+(z, 2k, \boldsymbol{\kappa}) + n_{\boldsymbol{q}}\widehat{C}^-(z, 2k, \boldsymbol{\kappa}) + (n_{\boldsymbol{p}} + n_{\boldsymbol{q}})\widehat{C}(z, 0, \boldsymbol{\kappa})]\, \mathrm{d}\boldsymbol{\kappa} W_{\boldsymbol{p},\boldsymbol{q}} \\
&- \int \widehat{C}(z, 0, \boldsymbol{\kappa})\left[\sum_{j=1}^{n_p} W_{\boldsymbol{p}|\{j|(\boldsymbol{\kappa}_p(j)-\boldsymbol{\kappa},\boldsymbol{\kappa}'_p(j)-\boldsymbol{\kappa})\},\boldsymbol{q}} + \sum_{l=1}^{n_q} W_{\boldsymbol{p},\boldsymbol{q}|\{l|(\boldsymbol{\kappa}_q(l)-\boldsymbol{\kappa},\boldsymbol{\kappa}'_q(l)-\boldsymbol{\kappa})}\right] \mathrm{d}\boldsymbol{\kappa} \\
&- \sum_{j_1\neq j_2=1}^{n_p}\int \Big\{\widehat{C}(z, 2k, \boldsymbol{\kappa}_p(j_1) - \boldsymbol{\kappa}'_p(j_1)) W_{\boldsymbol{p}|\{j_1,j_2|(\boldsymbol{\kappa}_p(j_2),\boldsymbol{\kappa}-\boldsymbol{\kappa}_p(j_1)),(\boldsymbol{\kappa}-\boldsymbol{\kappa}'_p(j_1),\boldsymbol{\kappa}'_p(j_2))\},\boldsymbol{q}} \\
&+ \frac{1}{2}\widehat{C}(z, 0, \boldsymbol{\kappa})[W_{\boldsymbol{p}|\{j_1,j_2|(\boldsymbol{\kappa}_p(j_1)-\boldsymbol{\kappa},\boldsymbol{\kappa}'_p(j_1)),(\boldsymbol{\kappa}_p(j_2)+\boldsymbol{\kappa},\boldsymbol{\kappa}'_p(j_2))\},\boldsymbol{q}} \\
&+ 2W_{\boldsymbol{p}|\{j_1,j_2|(\boldsymbol{\kappa}_p(j_1)-\boldsymbol{\kappa},\boldsymbol{\kappa}'_p(j_1)),(\boldsymbol{\kappa}_p(j_2),\boldsymbol{\kappa}'_p(j_2)-\boldsymbol{\kappa})\},\boldsymbol{q}} \\
&+ W_{\boldsymbol{p}|\{j_1,j_2|(\boldsymbol{\kappa}_p(j_1),\boldsymbol{\kappa}'_p(j_1)-\boldsymbol{\kappa}),(\boldsymbol{\kappa}_p(j_2),\boldsymbol{\kappa}'_p(j_2)+\boldsymbol{\kappa})\},\boldsymbol{q}}]\Big\}\, \mathrm{d}\boldsymbol{\kappa} \\
&- \sum_{l_1\neq l_2=1}^{n_q}\int \Big\{\hat{C}(z, 2k, \boldsymbol{\kappa}_q(l_1) - \boldsymbol{\kappa}'_q(l_1)) W_{\boldsymbol{p},\boldsymbol{q}|\{l_1,l_2|(\boldsymbol{\kappa}_q(l_2),\boldsymbol{\kappa}-\boldsymbol{\kappa}_q(l_1)),(\boldsymbol{\kappa}-\boldsymbol{\kappa}'_q(l_1),\boldsymbol{\kappa}'_q(l_2))\}} \\
&+ \frac{1}{2}\widehat{C}(z, 0, \boldsymbol{\kappa})[W_{\boldsymbol{p},\boldsymbol{q}|\{l_1,l_2|(\boldsymbol{\kappa}_q(l_1)-\boldsymbol{\kappa},\boldsymbol{\kappa}'_q(l_1)),(\boldsymbol{\kappa}_q(l_2)+\boldsymbol{\kappa},\boldsymbol{\kappa}'_q(l_2))\}}
\end{aligned}$$

$$
\begin{aligned}
&+2W_{\boldsymbol{p},\boldsymbol{q}|\{l_1,l_2|(\boldsymbol{\kappa}_q(l_1)-\boldsymbol{\kappa},\boldsymbol{\kappa}'_q(l_1)),(\boldsymbol{\kappa}_q(l_2),\boldsymbol{\kappa}'_q(l_2)-\boldsymbol{\kappa})\}}\\
&+W_{\boldsymbol{p},\boldsymbol{q}|\{l_1,l_2|(\boldsymbol{\kappa}_q(l_1),\boldsymbol{\kappa}'_q(l_1)-\boldsymbol{\kappa}),(\boldsymbol{\kappa}_q(l_2),\boldsymbol{\kappa}'_q(l_2)+\boldsymbol{\kappa})\}}]\Big\}\,\mathrm{d}\boldsymbol{\kappa}\\
&+\sum_{j=1}^{n_p}\sum_{l=1}^{n_q}\Big\{\widehat{C}(z,2k,\boldsymbol{\kappa}_p(j)-\boldsymbol{\kappa}'_p(j))\delta\big(\boldsymbol{\kappa}_p(j)-\boldsymbol{\kappa}'_p(j)-\boldsymbol{\kappa}_q(l)+\boldsymbol{\kappa}'_q(l)\big)W_{\boldsymbol{p}|j,\boldsymbol{q}|l}\\
&+\int\widehat{C}(z,0,\boldsymbol{\kappa})[W_{\boldsymbol{p}|\{j|(\boldsymbol{\kappa}_p(j)-\boldsymbol{\kappa},\boldsymbol{\kappa}'_p(j))\},\boldsymbol{q}|\{l|(\boldsymbol{\kappa}_q(l)-\boldsymbol{\kappa},\boldsymbol{\kappa}'_q(l))\}}\\
&+W_{\boldsymbol{p}|\{j|(\boldsymbol{\kappa}_p(j),\boldsymbol{\kappa}'_p(j)-\boldsymbol{\kappa})\},\boldsymbol{q}|\{l|(\boldsymbol{\kappa}_q(l),\boldsymbol{\kappa}'_q(l)-\boldsymbol{\kappa})\}}+W_{\boldsymbol{p}|\{j|(\boldsymbol{\kappa}_p(j)-\boldsymbol{\kappa},\boldsymbol{\kappa}'_p(j))\},\boldsymbol{q}|\{l|(\boldsymbol{\kappa}_q(l),\boldsymbol{\kappa}'_q(l)+\boldsymbol{\kappa})\}}\\
&+W_{\boldsymbol{p}|\{j|(\boldsymbol{\kappa}_p(j),\boldsymbol{\kappa}'_p(j)-\boldsymbol{\kappa})\},\boldsymbol{q}|\{l|(\boldsymbol{\kappa}_q(l)+\boldsymbol{\kappa},\boldsymbol{\kappa}'_q(l))\}}]\,\mathrm{d}\boldsymbol{\kappa}\\
&+\iiint\widehat{C}(z,2k,\boldsymbol{\kappa}_1)W_{\boldsymbol{p}|\{j|(\boldsymbol{\kappa}_p(j),\boldsymbol{\kappa}_2),(\boldsymbol{\kappa}_2-\boldsymbol{\kappa}_1,\boldsymbol{\kappa}'_p(j))\},\boldsymbol{q}|\{l|(\boldsymbol{\kappa}_q(l),\boldsymbol{\kappa}_3),(\boldsymbol{\kappa}_3-\boldsymbol{\kappa}_1,\boldsymbol{\kappa}'_q(l))\}}\mathrm{d}\boldsymbol{\kappa}_1\,\mathrm{d}\boldsymbol{\kappa}_2\,\mathrm{d}\boldsymbol{\kappa}_3\Big\},
\end{aligned}
$$

where $k=\omega/c_0(z)$ *and we have used the notations:*

$$
\begin{aligned}
&\boldsymbol{p}|j=\{(\boldsymbol{\kappa}_p(j'),\boldsymbol{\kappa}'_p(j'))\}_{j'=1\neq j}^{n_p},\\
&\boldsymbol{p}|\{j|(\boldsymbol{\kappa}_1,\boldsymbol{\kappa}_2)\}=\{(\boldsymbol{\kappa}_p(j'),\boldsymbol{\kappa}'_p(j'))\}_{j'=1\neq j}^{n_p}\cup(\boldsymbol{\kappa}_1,\boldsymbol{\kappa}_2).
\end{aligned}
$$

The proof of the proposition follows exactly that of [8] in which the medium was not absorbing and had no slow variation of the background velocity and impedance.

In the weak backscattering regime (24), we have

$$
W_{\boldsymbol{p},\boldsymbol{q}}=\begin{cases}\mathcal{O}(1) & \text{if}\quad n_{\boldsymbol{p}}=n_{\boldsymbol{q}}=0,\\ \mathcal{O}(\delta) & \text{if}\quad n_{\boldsymbol{p}}=n_{\boldsymbol{q}}=1,\\ \mathcal{O}(\delta^2) & \text{otherwise.}\end{cases}
$$

We have up to terms of order δ^2:

$$
\begin{aligned}
\frac{\partial W_{(\boldsymbol{\kappa}_1,\boldsymbol{\kappa}_2),(\boldsymbol{\kappa}_3,\boldsymbol{\kappa}_4)}}{\partial z}+\frac{2}{c_0(z)}\frac{\partial W_{(\boldsymbol{\kappa}_1,\boldsymbol{\kappa}_2),(\boldsymbol{\kappa}_3,\boldsymbol{\kappa}_4)}}{\partial\tau}&=-\frac{2\gamma_0(z)}{\zeta_0(z)}W_{(\boldsymbol{\kappa}_1,\boldsymbol{\kappa}_2),(\boldsymbol{\kappa}_3,\boldsymbol{\kappa}_4)}\\
&+\frac{\mathrm{i}c_0(z)}{2\omega}[(|\boldsymbol{\kappa}_3|^2+|\boldsymbol{\kappa}_4|^2)-(|\boldsymbol{\kappa}_1|^2+|\boldsymbol{\kappa}_2|^2)]W_{(\boldsymbol{\kappa}_1,\boldsymbol{\kappa}_2),(\boldsymbol{\kappa}_3,\boldsymbol{\kappa}_4)}\\
&+\frac{\omega^2}{4(2\pi)^d c_0^2(z)}\int\widehat{C}(z,0,\boldsymbol{\kappa})\{W_{(\boldsymbol{\kappa}_1-\boldsymbol{\kappa},\boldsymbol{\kappa}_2),(\boldsymbol{\kappa}_3-\boldsymbol{\kappa},\boldsymbol{\kappa}_4)}+W_{(\boldsymbol{\kappa}_1,\boldsymbol{\kappa}_2-\boldsymbol{\kappa}),(\boldsymbol{\kappa}_3,\boldsymbol{\kappa}_4-\boldsymbol{\kappa})}\\
&+W_{(\boldsymbol{\kappa}_1-\boldsymbol{\kappa},\boldsymbol{\kappa}_2),(\boldsymbol{\kappa}_3,\boldsymbol{\kappa}_4+\boldsymbol{\kappa})}+W_{(\boldsymbol{\kappa}_1,\boldsymbol{\kappa}_2-\boldsymbol{\kappa}),(\boldsymbol{\kappa}_3+\boldsymbol{\kappa},\boldsymbol{\kappa}_4)}\\
&-W_{(\boldsymbol{\kappa}_1-\boldsymbol{\kappa},\boldsymbol{\kappa}_2-\boldsymbol{\kappa}),(\boldsymbol{\kappa}_3,\boldsymbol{\kappa}_4)}-W_{(\boldsymbol{\kappa}_1,\boldsymbol{\kappa}_2),(\boldsymbol{\kappa}_3-\boldsymbol{\kappa},\boldsymbol{\kappa}_4-\boldsymbol{\kappa})}-2W_{(\boldsymbol{\kappa}_1,\boldsymbol{\kappa}_2),(\boldsymbol{\kappa}_3,\boldsymbol{\kappa}_4)}\}\,\mathrm{d}\boldsymbol{\kappa}\\
&+\frac{\omega^2}{4(2\pi)^d c_0^2(z)}\widehat{C}\left(z,\frac{2\omega}{c_0(z)},\boldsymbol{\kappa}_1-\boldsymbol{\kappa}_2\right)\delta(\boldsymbol{\kappa}_1-\boldsymbol{\kappa}_2-\boldsymbol{\kappa}_3+\boldsymbol{\kappa}_4)\delta(\tau),
\end{aligned}
\tag{A.6}
$$

with $W_{(\boldsymbol{\kappa}_1,\boldsymbol{\kappa}_2),(\boldsymbol{\kappa}_3,\boldsymbol{\kappa}_4)}(\omega,\tau,z=0)=0$. Note that the coupling terms preserve the sum $\boldsymbol{\kappa}_1-\boldsymbol{\kappa}_2-\boldsymbol{\kappa}_3+\boldsymbol{\kappa}_4$. Therefore $W_{(\boldsymbol{\kappa}_1,\boldsymbol{\kappa}_2),(\boldsymbol{\kappa}_3,\boldsymbol{\kappa}_4)}$ is supported on $\boldsymbol{\kappa}_1-\boldsymbol{\kappa}_2-\boldsymbol{\kappa}_3+\boldsymbol{\kappa}_4=\mathbf{0}$ and we can write the solution in terms of three 'effective' wave vectors. By parameterizing the remaining three wave vectors in a suitable form we obtain the statement of proposition 3.1. The density V is symmetric in $(\boldsymbol{\kappa}_u,\boldsymbol{\kappa}_v)$: $V_{\boldsymbol{\kappa}_u,\boldsymbol{\kappa}_v,\boldsymbol{\kappa}_w}(\omega,\tau,z)=V_{\boldsymbol{\kappa}_v,\boldsymbol{\kappa}_u,\boldsymbol{\kappa}_w}(\omega,\tau,z)$. This can be seen from the structure of the system (27) in proposition 3.1, and this also follows directly from the reciprocity relation $\hat{\mathcal{R}}^\varepsilon(\boldsymbol{\kappa},\boldsymbol{\kappa}')=\hat{\mathcal{R}}^\varepsilon(-\boldsymbol{\kappa}',-\boldsymbol{\kappa})$.

Appendix B. The system for the dimensionless density

In this appendix, we introduce a dimensionless formulation of the system of equations that determines the cross spectral density V defined in proposition 3.1. The autocorrelation

function C of the fluctuations of the medium is defined by (6). We introduce the dimensionless autocorrelation function $\mathcal{C}$ of the random medium:

$$C(z, z', \boldsymbol{x}') = \sigma^2 \mathcal{C}\left(\frac{z}{L}, \frac{z'}{l_z}, \frac{\boldsymbol{x}'}{l_x}\right),$$

where l_z (respectively l_x) is the longitudinal (respectively transverse) correlation radius of the random fluctuations and σ is the standard deviation of the fluctuations. We denote by $\widehat{\mathcal{C}}(\tilde{z}, K, \boldsymbol{\mu})$ and by $\check{\mathcal{C}}(\tilde{z}, K, \boldsymbol{\lambda})$ the full and partial Fourier transforms

$$\widehat{\mathcal{C}}(\tilde{z}, K, \boldsymbol{\mu}) = \int\int_{-\infty}^{\infty} \mathcal{C}(\tilde{z}, \tilde{z}', \boldsymbol{\lambda})\, \mathrm{e}^{-\mathrm{i}K\tilde{z}' - \mathrm{i}\boldsymbol{\mu}\cdot\boldsymbol{\lambda}}\, \mathrm{d}\tilde{z}'\, \mathrm{d}\boldsymbol{\lambda}, \tag{B.1}$$

$$\check{\mathcal{C}}(\tilde{z}, K, \boldsymbol{\lambda}) = \int_{-\infty}^{\infty} \mathcal{C}(\tilde{z}, \tilde{z}', \boldsymbol{\lambda})\, \mathrm{e}^{-\mathrm{i}K\tilde{z}'} \mathrm{d}\tilde{z}'. \tag{B.2}$$

We introduce the dimensionless profiles $\tilde{c}_0(\tilde{z})$, $\tilde{\zeta}_0(\tilde{z})$, and $\tilde{\gamma}_0(\tilde{z})$:

$$c_0(z) = \bar{c}\tilde{c}_0\left(\frac{z}{L}\right), \qquad \zeta_0(z) = \bar{\zeta}\tilde{\zeta}_0\left(\frac{z}{L}\right), \qquad \gamma_0(z) = \bar{\gamma}\tilde{\gamma}_0\left(\frac{z}{L}\right), \tag{B.3}$$

where $\bar{c}$, $\bar{\zeta}$ and $\bar{\gamma}$ are typical speed of sound, impedance and absorption coefficients. We also define the dimensionless functions

$$\tilde{J}_0(\tilde{z}) = \int_0^{\tilde{z}} \tilde{c}_0(\tilde{z}')\, \mathrm{d}\tilde{z}', \qquad \tilde{G}_0(\tilde{z}) = \int_0^{\tilde{z}} \frac{\tilde{\gamma}_0(\tilde{z}')}{\tilde{\zeta}_0(\tilde{z}')}\, \mathrm{d}\tilde{z}', \qquad \tilde{\tau}_0(\tilde{z}) = \int_0^{\tilde{z}} \frac{1}{\tilde{c}_0(\tilde{z}')}\, \mathrm{d}\tilde{z}'. \tag{B.4}$$

We consider the Fourier transform D of the cross spectral density V

$$V_{\boldsymbol{\kappa}_u, \boldsymbol{\kappa}_v, \boldsymbol{\kappa}_w}(\omega, \tau, z) = \frac{1}{2\pi} \int D(\omega, h, z, \boldsymbol{\kappa}_u, \boldsymbol{\kappa}_v, \boldsymbol{\kappa}_w)\, \mathrm{e}^{-\mathrm{i}h\tau}\, \mathrm{d}h. \tag{B.5}$$

The following proposition shows that the parameters α and β defined by (28) determine the evolution of D.

Proposition B.1. *The density D is given by*

$$\begin{aligned} D(\omega, h, z, \boldsymbol{\kappa}_u, \boldsymbol{\kappa}_v, \boldsymbol{\kappa}_w) &= \bar{D}\mathcal{D}\left(\frac{\omega}{\omega_0}, \frac{hL}{\bar{c}}, \frac{z}{L}, \boldsymbol{\kappa}_u l_x, \boldsymbol{\kappa}_v l_x, \boldsymbol{\kappa}_w l_x\right) \\ &\quad \times \exp\left[2\mathrm{i}\frac{hL}{\bar{c}}\tilde{\tau}_0\left(\frac{z}{L}\right) - \bar{G}\tilde{G}_0\left(\frac{z}{L}\right) - \mathrm{i}\boldsymbol{\kappa}_u \cdot \boldsymbol{\kappa}_v \frac{\bar{c}L}{\omega}\tilde{J}_0\left(\frac{z}{L}\right)\right], \end{aligned} \tag{B.6}$$

with

$$\bar{D} = \frac{\omega_0^2 \sigma^2 l_z l_x^d L}{4(2\pi)^d \bar{c}^2}, \qquad \bar{G} = \frac{2\bar{\sigma}L}{\bar{\zeta}}.$$

The frequencies $\tilde{\omega}$ and $\tilde{h}$ are frozen parameters in the equation satisfied by the dimensionless density $\mathcal{D}(\tilde{\omega}, \tilde{h}, \tilde{z}, \boldsymbol{u}, \boldsymbol{v}, \boldsymbol{w})$:

$$\begin{aligned} \frac{\mathrm{d}\mathcal{D}(\tilde{\omega}, \tilde{h}, \tilde{z}, \boldsymbol{u}, \boldsymbol{v}, \boldsymbol{w})}{\mathrm{d}\tilde{z}} &= \tilde{\omega}^2 \widehat{\mathcal{B}}_{2\tilde{\omega}}(\tilde{z}, \boldsymbol{w})\, \mathrm{e}^{\mathrm{i}\frac{\alpha}{\tilde{\omega}}\boldsymbol{u}\cdot\boldsymbol{v}\tilde{J}_0(\tilde{z})}\, \mathrm{e}^{-2\mathrm{i}\tilde{h}\tilde{\tau}_0(\tilde{z})}\, \mathrm{e}^{\bar{G}\tilde{G}_0(\tilde{z})} + \frac{\beta\tilde{\omega}^2}{(2\pi)^d} \int \widehat{\mathcal{B}}_0(\tilde{z}, \boldsymbol{\mu}) \\ &\quad \times [\mathrm{e}^{\mathrm{i}\frac{\alpha}{\tilde{\omega}}\boldsymbol{\mu}\cdot\boldsymbol{v}\tilde{J}_0(\tilde{z})}\mathcal{D}(\tilde{\omega}, \tilde{h}, \tilde{z}, \boldsymbol{u} - \boldsymbol{\mu}, \boldsymbol{v}, \boldsymbol{w} + \boldsymbol{\mu}) + \mathrm{e}^{-\mathrm{i}\frac{\alpha}{\tilde{\omega}}\boldsymbol{\mu}\cdot\boldsymbol{v}\tilde{J}_0(\tilde{z})}\mathcal{D}(\tilde{\omega}, \tilde{h}, \tilde{z}, \boldsymbol{u} + \boldsymbol{\mu}, \boldsymbol{v}, \boldsymbol{w} + \boldsymbol{\mu}) \\ &\quad + \mathrm{e}^{\mathrm{i}\frac{\alpha}{\tilde{\omega}}\boldsymbol{\mu}\cdot\boldsymbol{u}\tilde{J}_0(\tilde{z})}\mathcal{D}(\tilde{\omega}, \tilde{h}, \tilde{z}, \boldsymbol{u}, \boldsymbol{v} - \boldsymbol{\mu}, \boldsymbol{w} + \boldsymbol{\mu}) + \mathrm{e}^{-\mathrm{i}\frac{\alpha}{\tilde{\omega}}\boldsymbol{\mu}\cdot\boldsymbol{u}\tilde{J}_0(\tilde{z})}\mathcal{D}(\tilde{\omega}, \tilde{h}, \tilde{z}, \boldsymbol{u}, \boldsymbol{v} + \boldsymbol{\mu}, \boldsymbol{w} + \boldsymbol{\mu}) \\ &\quad - \mathrm{e}^{-\mathrm{i}\frac{\alpha}{\tilde{\omega}}[\boldsymbol{\mu}\cdot\boldsymbol{u} + \boldsymbol{\mu}\cdot(\boldsymbol{v}+\boldsymbol{\mu})]\tilde{J}_0(\tilde{z})}\mathcal{D}(\tilde{\omega}, \tilde{h}, \tilde{z}, \boldsymbol{u} + \boldsymbol{\mu}, \boldsymbol{v} + \boldsymbol{\mu}, \boldsymbol{w}) \\ &\quad - \mathrm{e}^{-\mathrm{i}\frac{\alpha}{\tilde{\omega}}[\boldsymbol{\mu}\cdot\boldsymbol{u} - \boldsymbol{\mu}\cdot(\boldsymbol{v}+\boldsymbol{\mu})]\tilde{J}_0(\tilde{z})}\mathcal{D}(\tilde{\omega}, \tilde{h}, \tilde{z}, \boldsymbol{u} - \boldsymbol{\mu}, \boldsymbol{v} + \boldsymbol{\mu}, \boldsymbol{w}) - 2\mathcal{D}(\tilde{\omega}, \tilde{h}, \tilde{z}, \boldsymbol{u}, \boldsymbol{v}, \boldsymbol{w})]\, \mathrm{d}\boldsymbol{\mu}, \end{aligned} \tag{B.7}$$

starting from $\mathcal{D}(\tilde{z} = 0, \boldsymbol{u}, \boldsymbol{v}, \boldsymbol{w}) = 0$, where

$$\widehat{\mathcal{B}}_{\tilde{\omega}}(\tilde{z}, \boldsymbol{w}) = \frac{1}{\tilde{c}_0^2(\tilde{z})}\widehat{\mathcal{C}}\left(\tilde{z}, \frac{\omega_0 l_z}{\bar{c}\tilde{c}_0(\tilde{z})}\tilde{\omega}, \boldsymbol{w}\right). \tag{B.8}$$

Appendix C. Proof of proposition 4.1

The mean reflected intensity $I^\varepsilon(t)$ has the limit $I(t)$ as $\varepsilon \to 0$:

$$I(t) = \frac{1}{(2\pi)^{d+1}} \int \cdots \int W_{(\boldsymbol{\kappa}_1,\boldsymbol{\kappa}_2),(\boldsymbol{\kappa}_1,\boldsymbol{\kappa}_4)}(\omega, t, L)\hat{b}_{\rm s}(\omega, \boldsymbol{\kappa}_2)\overline{\hat{b}_{\rm s}}(\omega, \boldsymbol{\kappa}_4)\, {\rm d}\boldsymbol{\kappa}_1\, {\rm d}\boldsymbol{\kappa}_2\, {\rm d}\boldsymbol{\kappa}_4\, {\rm d}\omega.$$

Using identity (B.6), this can be expressed as

$$\begin{aligned} I(t) &= \frac{1}{(2\pi)^{d+1}} \int \cdots \int D(\omega, h, L, \mathbf{0}, \boldsymbol{\kappa} + 2\boldsymbol{\kappa}', \boldsymbol{\kappa})\, {\rm d}\boldsymbol{\kappa}\, {\rm e}^{-{\rm i}ht} |\hat{b}_{\rm s}(\omega, \boldsymbol{\kappa}')|^2\, {\rm d}\boldsymbol{\kappa}'\, {\rm d}h\, {\rm d}\omega \\ &= \frac{\bar{D}}{(2\pi)^{d+2}} \iiint \mathcal{E}\left(\frac{\omega}{\omega_0}, \frac{hL}{\bar{c}}, 1, 2\boldsymbol{\kappa}' l_x\right) {\rm e}^{2{\rm i}\frac{hL}{\bar{c}}\tilde{\tau}_0(1) - {\rm i}ht} {\rm e}^{-\bar{G}\tilde{G}_0(1)} |\hat{b}_{\rm s}(\omega, \boldsymbol{\kappa}')|^2\, {\rm d}\boldsymbol{\kappa}'\, {\rm d}h\, {\rm d}\omega, \end{aligned} \tag{C.1}$$

where

$$\mathcal{E}(\tilde{\omega}, \tilde{h}, \tilde{z}, \boldsymbol{v}) = \int \mathcal{D}(\tilde{\omega}, \tilde{h}, \tilde{z}, \mathbf{0}, \boldsymbol{w} + 2\boldsymbol{v}, \boldsymbol{w})\, {\rm d}\boldsymbol{w}.$$

Then, using the system of coupled differential equations (B.7), we get that the quantity $\mathcal{E}(\tilde{\omega}, \tilde{h}, \tilde{z}, \boldsymbol{v})$ satisfies the differential equation

$$\begin{aligned} \frac{{\rm d}\mathcal{E}(\tilde{\omega}, \tilde{h}, \tilde{z}, \boldsymbol{v})}{{\rm d}\tilde{z}} &= (2\pi)^d \tilde{\omega}^2 \check{\mathcal{B}}_{2\tilde{\omega}}(\tilde{z}, \mathbf{0})\, {\rm e}^{\bar{G}\tilde{G}_0(\tilde{z})}\, {\rm e}^{-2{\rm i}\tilde{h}\tilde{\tau}_0(\tilde{z})} \\ &\quad + \frac{\beta\tilde{\omega}^2}{(2\pi)^d} \int \widehat{\mathcal{B}}_0(\tilde{z}, \boldsymbol{\mu})[\mathcal{E}(\tilde{\omega}, \tilde{h}, \tilde{z}, \boldsymbol{v} + \boldsymbol{\mu}) - \mathcal{E}(\tilde{\omega}, \tilde{h}, \tilde{z}, \boldsymbol{v})]\, {\rm d}\boldsymbol{\mu}, \end{aligned}$$

because all but two terms proportional to β on the right-hand side of (B.6) cancel each other when taking $(\boldsymbol{u}, \boldsymbol{v}, \boldsymbol{w}) \to (\mathbf{0}, \boldsymbol{w} + 2\boldsymbol{v}, \boldsymbol{w})$ and integrating in $\boldsymbol{w}$. Here $\check{\mathcal{B}}_{\tilde{\omega}}(\tilde{z}, \boldsymbol{\lambda})$ is the inverse Fourier transform of $\widehat{\mathcal{B}}_{\tilde{\omega}}(\tilde{z}, \boldsymbol{w})$:

$$\check{\mathcal{B}}_{\tilde{\omega}}(\tilde{z}, \boldsymbol{\lambda}) = \frac{1}{\tilde{c}_0^2(\tilde{z})} \check{\mathcal{C}}\left(\tilde{z}, \frac{\omega_0 l_z}{\bar{c}\tilde{c}_0(\tilde{z})}\tilde{\omega}, \boldsymbol{\lambda}\right). \tag{C.2}$$

The initial condition for the differential equation for $\mathcal{E}$ is $\mathcal{E}(\tilde{\omega}, \tilde{h}, \tilde{z} = 0, \boldsymbol{v}) = 0$. The solution is the function

$$\mathcal{E}(\tilde{\omega}, \tilde{h}, \tilde{z}, \boldsymbol{v}) = (2\pi)^d \tilde{\omega}^2 \int_0^{\tilde{z}} \check{\mathcal{B}}_{2\tilde{\omega}}(\tilde{z}', \mathbf{0})\, {\rm e}^{\bar{G}\tilde{G}_0(\tilde{z}')}\, {\rm e}^{-2{\rm i}\tilde{h}\tilde{\tau}_0(\tilde{z}')}\, {\rm d}\tilde{z}',$$

which is independent of $\boldsymbol{v}$. We next substitute in (C.1) and integrate with respect to h. The integral in h generates a delta distribution:

$$\begin{aligned} I(t) = \frac{\bar{D}}{2\pi l_x^d} \int\int_0^1 \delta\left(t - \frac{2L}{\bar{c}}(\tilde{\tau}_0(1) - \tilde{\tau}_0(\tilde{z}))\right) \frac{\omega^2}{\omega_0^2} \check{\mathcal{B}}_{2\frac{\omega}{\omega_0}}(\tilde{z}, \mathbf{0}) \\ \times {\rm e}^{\bar{G}(\tilde{G}_0(\tilde{z}) - \tilde{G}_0(1))} \left[\int |\hat{b}_{\rm s}(\omega, \boldsymbol{\kappa}')|^2\, {\rm d}\boldsymbol{\kappa}'\right] {\rm d}\tilde{z}\, {\rm d}\omega. \end{aligned}$$

The delta distribution concentrates the integrand on a particular value of $\tilde{z}$:

$$I(t) = \frac{\bar{D}\bar{c}}{4\pi l_x^d L} \int \tilde{c}_0(\tilde{z}(t)) \frac{\omega^2}{\omega_0^2} \check{\mathcal{B}}_{2\frac{\omega}{\omega_0}}(\tilde{z}(t), \mathbf{0})\, {\rm e}^{\bar{G}(\tilde{G}_0(\tilde{z}(t)) - \tilde{G}_0(1))} \left[\int |\hat{b}_{\rm s}(\omega, \boldsymbol{\kappa}')|^2\, {\rm d}\boldsymbol{\kappa}'\right] {\rm d}\omega,$$

where $\tilde{z}(t) \in (0, 1)$ is such that

$$\int_{\tilde{z}(t)}^L \frac{1}{\tilde{c}_0(\tilde{z}')}\, {\rm d}\tilde{z}' = \frac{\bar{c}t}{2L}. \tag{C.3}$$

The expression of the intensity in the original variables is given by (31).

Appendix D. Asymptotic expressions for the cross spectral density

In the following two lemmas we give the asymptotic expressions for the dimensionless density $\mathcal{D}$ in the regime $\alpha \gg 1$. They generalize the results obtained in [8].

Lemma D.1.

(i) *If* $\boldsymbol{u}\cdot\boldsymbol{v} \neq 0$, *then* $\lim_{\alpha\to\infty} \mathcal{D}(\tilde{z}, \boldsymbol{u}, \boldsymbol{v}, \boldsymbol{w}) = 0$.

(ii) *If* $\boldsymbol{u} \neq \mathbf{0}$, $\boldsymbol{v} \neq \mathbf{0}$, *and* $\boldsymbol{u}\cdot\boldsymbol{v} = 0$, *then*

$$\lim_{\alpha\to\infty} \mathcal{D}(\tilde{z}, \tilde{\omega}, \tilde{h}, \boldsymbol{u}, \boldsymbol{v}, \boldsymbol{w}) = \int_0^{\tilde{z}} \tilde{\omega}^2 \widehat{\mathcal{B}}_{2\tilde{\omega}}(\tilde{z}', \boldsymbol{w})\, \mathrm{e}^{-2\mathrm{i}\tilde{h}\tilde{\tau}_0(\tilde{z}')}\, \mathrm{e}^{\bar{G}\tilde{G}_0(\tilde{z}')}\, \mathrm{e}^{-2\beta\tilde{\omega}^2 \int_{\tilde{z}'}^{\tilde{z}} \check{\mathcal{B}}_0(\tilde{z}'', \mathbf{0})\, \mathrm{d}\tilde{z}''} \mathrm{d}\tilde{z}'. \tag{D.1}$$

(iii) *If* $\boldsymbol{u} = \mathbf{0}$ *and* $\boldsymbol{v} \neq \mathbf{0}$, *then* $\lim_{\alpha\to\infty} \mathcal{D}(\tilde{z}, \tilde{\omega}, \tilde{h}, \mathbf{0}, \boldsymbol{v}, \boldsymbol{w}) = \mathcal{D}_{\mathbf{0}}(\tilde{z}, \tilde{\omega}, \tilde{h}, \boldsymbol{w})$ *where* $\mathcal{D}_{\mathbf{0}}(\tilde{z}, \tilde{\omega}, \tilde{h}, \boldsymbol{w})$ *is the solution of*

$$\frac{\mathrm{d}\mathcal{D}_{\mathbf{0}}}{\mathrm{d}\tilde{z}} = \tilde{\omega}^2 \widehat{\mathcal{B}}_{2\tilde{\omega}}(\tilde{z}, \boldsymbol{w})\, \mathrm{e}^{-2\mathrm{i}\tilde{h}\tilde{\tau}_0(\tilde{z})}\, \mathrm{e}^{\bar{G}\tilde{G}_0(\tilde{z})} + \frac{2\beta\tilde{\omega}^2}{(2\pi)^d} \int \widehat{\mathcal{B}}_0(\tilde{z}, \boldsymbol{\mu}) \left[\mathcal{D}_{\mathbf{0}}(\boldsymbol{w}+\boldsymbol{\mu}) - \mathcal{D}_{\mathbf{0}}(\boldsymbol{w})\right] \mathrm{d}\boldsymbol{\mu}, \tag{D.2}$$

starting from $\mathcal{D}_{\mathbf{0}}(\tilde{z} = 0, \tilde{\omega}, \tilde{h}, \boldsymbol{w}) = 0$.

(iv) *If* $\boldsymbol{u} \neq \mathbf{0}$ *and* $\boldsymbol{v} = \mathbf{0}$, *then* $\lim_{\alpha\to\infty} \mathcal{D}(\tilde{z}, \tilde{\omega}, \tilde{h}, \boldsymbol{u}, \mathbf{0}, \boldsymbol{w}) = \mathcal{D}_{\mathbf{0}}(\tilde{z}, \tilde{\omega}, \tilde{h}, \boldsymbol{w})$.

(v) *If* $\boldsymbol{u} = \mathbf{0}$ *and* $\boldsymbol{v} = \mathbf{0}$, *then*

$$\lim_{\alpha\to\infty} \mathcal{D}(\tilde{z}, \tilde{\omega}, \tilde{h}, \mathbf{0}, \mathbf{0}, \boldsymbol{w}) = 2\mathcal{D}_{\mathbf{0}}(\tilde{z}, \tilde{\omega}, \tilde{h}, \boldsymbol{w}) - \int_0^{\tilde{z}} \tilde{\omega}^2 \widehat{\mathcal{B}}_{2\tilde{\omega}}(\tilde{z}', \boldsymbol{w})\, \mathrm{e}^{-2\mathrm{i}\tilde{h}\tilde{\tau}_0(\tilde{z}')}\, \mathrm{e}^{\bar{G}\tilde{G}_0(\tilde{z}')}\, \mathrm{e}^{-2\beta\tilde{\omega}^2 \int_{\tilde{z}'}^{\tilde{z}} \check{\mathcal{B}}_0(\tilde{z}'', \mathbf{0})\, \mathrm{d}\tilde{z}''} \mathrm{d}\tilde{z}'.$$

By comparing the second and third items (or the fourth and fifth items) a sharp transition is noted from the case $\boldsymbol{u} = \mathbf{0}$ to $\boldsymbol{u} \neq \mathbf{0}$. This transition can be studied in detail by looking at small $\boldsymbol{u}$ of order α^{-1}.

Lemma D.2.

(i) *If* $\boldsymbol{v} \neq \mathbf{0}$, *then* $\lim_{\alpha\to\infty} \mathcal{D}(\tilde{z}, \tilde{\omega}, \tilde{h}, \alpha^{-1}\boldsymbol{s}, \boldsymbol{v}, \boldsymbol{w}) = \mathcal{D}_{\boldsymbol{s}}(\tilde{z}, \tilde{\omega}, \tilde{h}, \boldsymbol{v}, \boldsymbol{w})$ *where* $\mathcal{D}_{\boldsymbol{s}}$ *is solution of*

$$\frac{\mathrm{d}\mathcal{D}_{\boldsymbol{s}}}{\mathrm{d}\tilde{z}} = \tilde{\omega}^2 \widehat{\mathcal{B}}_{2\tilde{\omega}}(\tilde{z}, \boldsymbol{w})\, \mathrm{e}^{-2\mathrm{i}\tilde{h}\tilde{\tau}_0(\tilde{z})}\, \mathrm{e}^{\bar{G}\tilde{G}_0(\tilde{z})}\, \mathrm{e}^{\mathrm{i}\boldsymbol{s}\cdot\boldsymbol{v}\frac{\tilde{J}_0(\tilde{z})}{\tilde{\omega}}} + \frac{\beta\tilde{\omega}^2}{(2\pi)^d} \int \widehat{\mathcal{B}}_0(\tilde{z}, \boldsymbol{\mu}) \times \left[\mathrm{e}^{\mathrm{i}\boldsymbol{s}\cdot\boldsymbol{\mu}\frac{\tilde{J}_0(\tilde{z})}{\tilde{\omega}}} \mathcal{D}_{\boldsymbol{s}}(\boldsymbol{v}-\boldsymbol{\mu}, \boldsymbol{w}+\boldsymbol{\mu}) + \mathrm{e}^{-\mathrm{i}\boldsymbol{s}\cdot\boldsymbol{\mu}\frac{\tilde{J}_0(\tilde{z})}{\tilde{\omega}}} \mathcal{D}_{\boldsymbol{s}}(\boldsymbol{v}+\boldsymbol{\mu}, \boldsymbol{w}+\boldsymbol{\mu}) - 2\mathcal{D}_{\boldsymbol{s}}(\boldsymbol{v}, \boldsymbol{w})\right] \mathrm{d}\boldsymbol{\mu}, \tag{D.3}$$

starting from $\mathcal{D}_{\boldsymbol{s}}(\tilde{z} = 0, \tilde{\omega}, \tilde{h}, \boldsymbol{v}, \boldsymbol{w}) = 0$.

(ii) *For any* $\boldsymbol{s}, \boldsymbol{s}'$, *we have*

$$\lim_{\alpha\to\infty} \mathcal{D}(\tilde{z}, \tilde{\omega}, \tilde{h}, \alpha^{-1}\boldsymbol{s}, \alpha^{-1}\boldsymbol{s}', \boldsymbol{w}) = \mathcal{D}_{\boldsymbol{s}}(\tilde{z}, \tilde{\omega}, \tilde{h}, \mathbf{0}, \boldsymbol{w}) + \mathcal{D}_{\boldsymbol{s}'}(\tilde{z}, \tilde{\omega}, \tilde{h}, \mathbf{0}, \boldsymbol{w}) - \int_0^{\tilde{z}} \tilde{\omega}^2 \widehat{\mathcal{B}}_{2\tilde{\omega}}(\tilde{z}', \boldsymbol{w})\, \mathrm{e}^{-2\mathrm{i}\tilde{h}\tilde{\tau}_0(\tilde{z}')}\, \mathrm{e}^{\bar{G}\tilde{G}_0(\tilde{z}')}\, \mathrm{e}^{-2\beta\tilde{\omega}^2 \int_{\tilde{z}'}^{\tilde{z}} \check{\mathcal{B}}_0(\tilde{z}'', \mathbf{0})\, \mathrm{d}\tilde{z}''} \mathrm{d}\tilde{z}'.$$

By solving the differential equation (D.3) we obtain the following integral representation of $\mathcal{D}_{\boldsymbol{s}}(\tilde{z}, \boldsymbol{v}, \boldsymbol{w})$ valid for all $\boldsymbol{s} \in \mathbb{R}^d$:

$$\mathcal{D}_{\boldsymbol{s}}(\tilde{z},\tilde{\omega},\tilde{h},\boldsymbol{v},\boldsymbol{w}) = \int\!\!\int_0^{\tilde{z}} \tilde{\omega}^2 \check{\mathcal{B}}_{2\tilde{\omega}}(\tilde{z}',\boldsymbol{\lambda})\, \mathrm{e}^{-2\mathrm{i}\tilde{h}\tilde{\tau}_0(\tilde{z}')}\, \mathrm{e}^{\bar{G}\tilde{G}_0(\tilde{z}')}\, \mathrm{e}^{-\mathrm{i}\boldsymbol{w}\cdot\boldsymbol{\lambda}}\, \mathrm{e}^{\mathrm{i}\boldsymbol{v}\cdot\boldsymbol{s}\frac{\tilde{J}_0(\tilde{z}')}{\tilde{\omega}}}$$
$$\times\, \mathrm{e}^{\beta\tilde{\omega}^2\int_{\tilde{z}'}^{\tilde{z}} \check{\mathcal{B}}_0(\tilde{z}'',\boldsymbol{\lambda}-\frac{\boldsymbol{s}}{\tilde{\omega}}[\tilde{J}_0(\tilde{z}'')-\tilde{J}_0(\tilde{z}')])+\check{\mathcal{B}}_0(\tilde{z}'',\boldsymbol{\lambda}+\frac{\boldsymbol{s}}{\tilde{\omega}}[\tilde{J}_0(\tilde{z}'')-\tilde{J}_0(\tilde{z}')])-2\check{\mathcal{B}}_0(\tilde{z}'',\boldsymbol{0})\,\mathrm{d}\tilde{z}''}\,\mathrm{d}\tilde{z}'\,\mathrm{d}\boldsymbol{\lambda}. \quad \text{(D.4)}$$

In the particular case in which $\boldsymbol{s}=\boldsymbol{0}$ the function $\mathcal{D}_{\boldsymbol{s}}$ is independent of $\boldsymbol{v}$ and we have

$$\lim_{\boldsymbol{s}\to\boldsymbol{0}} \mathcal{D}_{\boldsymbol{s}}(\tilde{z},\tilde{\omega},\tilde{h},\boldsymbol{v},\boldsymbol{w}) = \mathcal{D}_{\boldsymbol{0}}(\tilde{z},\tilde{\omega},\tilde{h},\boldsymbol{w})$$
$$= \int\!\!\int_0^{\tilde{z}} \tilde{\omega}^2 \check{\mathcal{B}}_{2\tilde{\omega}}(\tilde{z}',\boldsymbol{\lambda})\, \mathrm{e}^{-2\mathrm{i}\tilde{h}\tilde{\tau}_0(\tilde{z}')}\, \mathrm{e}^{\bar{G}\tilde{G}_0(\tilde{z}')}\, \mathrm{e}^{-\mathrm{i}\boldsymbol{w}\cdot\boldsymbol{\lambda}} \mathrm{e}^{2\beta\tilde{\omega}^2\int_{\tilde{z}'}^{\tilde{z}} \check{\mathcal{B}}_0(\tilde{z}'',\boldsymbol{\lambda})-\check{\mathcal{B}}_0(\tilde{z}'',\boldsymbol{0})]d\tilde{z}''}\mathrm{d}\tilde{z}'\,\mathrm{d}\boldsymbol{\lambda}.$$

We also have

$$\lim_{|\boldsymbol{s}|\to\infty} \mathcal{D}_{\boldsymbol{s}}(\tilde{z},\tilde{\omega},\tilde{h},\boldsymbol{0},\boldsymbol{w}) = \int_0^{\tilde{z}} \tilde{\omega}^2 \widehat{\mathcal{B}}_{2\tilde{\omega}}(\tilde{z}',\boldsymbol{w})\, \mathrm{e}^{-2\mathrm{i}\tilde{h}\tilde{\tau}_0(\tilde{z}')}\, \mathrm{e}^{\bar{G}\tilde{G}_0(\tilde{z}')}\, \mathrm{e}^{-2\beta\tilde{\omega}^2\int_{\tilde{z}'}^{\tilde{z}} \check{\mathcal{B}}_0(\tilde{z}'',\boldsymbol{0})\,\mathrm{d}\tilde{z}''}\mathrm{d}\tilde{z}'.$$

Appendix E. Proof of proposition 4.2

The beam width $R^\varepsilon(t)$ converges to $R(t)$ as $\varepsilon\to 0$, where $R(t)$ is given by

$$R^2(t) = -\frac{\int\cdots\int \Delta_{\boldsymbol{\kappa}_3} W_{(\boldsymbol{\kappa}_1,\boldsymbol{\kappa}_2),(\boldsymbol{\kappa}_3,\boldsymbol{\kappa}_4)}(\omega,t,L)|_{\boldsymbol{\kappa}_3=\boldsymbol{\kappa}_1}\hat{b}_{\mathrm{s}}(\omega,\boldsymbol{\kappa}_2)\overline{\hat{b}_{\mathrm{s}}}(\omega,\boldsymbol{\kappa}_4)\,\mathrm{d}\boldsymbol{\kappa}_1\,\mathrm{d}\boldsymbol{\kappa}_2\,\mathrm{d}\boldsymbol{\kappa}_4\,\mathrm{d}\omega}{\int\cdots\int W_{(\boldsymbol{\kappa}_1,\boldsymbol{\kappa}_2),(\boldsymbol{\kappa}_1,\boldsymbol{\kappa}_4)}(\omega,t,L)\hat{b}_{\mathrm{s}}(\omega,\boldsymbol{\kappa}_2)\overline{\hat{b}_{\mathrm{s}}}(\omega,\boldsymbol{\kappa}_4)d\boldsymbol{\kappa}_1\,\mathrm{d}\boldsymbol{\kappa}_2\,\mathrm{d}\boldsymbol{\kappa}_4\,\mathrm{d}\omega}$$
$$= \frac{\int\cdots\int D(\omega,h,L,\boldsymbol{0},\boldsymbol{\kappa}+2\boldsymbol{\kappa}',\boldsymbol{\kappa})\,\mathrm{e}^{-\mathrm{i}ht}|\nabla_{\boldsymbol{\kappa}'}\hat{b}_{\mathrm{s}}(\omega,\boldsymbol{\kappa}')|^2\,\mathrm{d}\boldsymbol{\kappa}\,\mathrm{d}\boldsymbol{\kappa}'\,\mathrm{d}h\,\mathrm{d}\omega}{\int\cdots\int D(\omega,h,L,\boldsymbol{0},\boldsymbol{\kappa}+2\boldsymbol{\kappa}',\boldsymbol{\kappa})\,\mathrm{e}^{-\mathrm{i}ht}|\hat{b}_{\mathrm{s}}(\omega,\boldsymbol{\kappa}')|^2\,\mathrm{d}\boldsymbol{\kappa}\,\mathrm{d}\boldsymbol{\kappa}'\,\mathrm{d}h\,\mathrm{d}\omega}$$
$$- \frac{\int\cdots\int(\Delta_{\boldsymbol{\kappa}_u}+\Delta_{\boldsymbol{\kappa}_v})D(\omega,h,L,\boldsymbol{0},\boldsymbol{\kappa}+2\boldsymbol{\kappa}',\boldsymbol{\kappa})\,\mathrm{e}^{-\mathrm{i}ht}|\hat{b}_{\mathrm{s}}(\omega,\boldsymbol{\kappa}')|^2\,\mathrm{d}\boldsymbol{\kappa}\,\mathrm{d}\boldsymbol{\kappa}'\,\mathrm{d}h\,\mathrm{d}\omega}{\int\cdots\int D(\omega,h,L,\boldsymbol{0},\boldsymbol{\kappa}+2\boldsymbol{\kappa}',\boldsymbol{\kappa})\,\mathrm{e}^{-\mathrm{i}ht}|\hat{b}_{\mathrm{s}}(\omega,\boldsymbol{\kappa}')|^2\,\mathrm{d}\boldsymbol{\kappa}\,\mathrm{d}\boldsymbol{\kappa}'\,\mathrm{d}h\,\mathrm{d}\omega}$$
$$+ \frac{\int\cdots\int 2\mathrm{i}\nabla_{\boldsymbol{\kappa}_u}D(\omega,h,L,\boldsymbol{0},\boldsymbol{\kappa}+2\boldsymbol{\kappa}',\boldsymbol{\kappa})\,\mathrm{e}^{-\mathrm{i}ht}\mathrm{Im}(\hat{b}_{\mathrm{s}}\overline{\nabla_{\boldsymbol{\kappa}'}\hat{b}_{\mathrm{s}}}(\omega,\boldsymbol{\kappa}'))\,\mathrm{d}\boldsymbol{\kappa}\,\mathrm{d}\boldsymbol{\kappa}'\,\mathrm{d}h\,\mathrm{d}\omega}{\int\cdots\int D(\omega,h,L,\boldsymbol{0},\boldsymbol{\kappa}+2\boldsymbol{\kappa}',\boldsymbol{\kappa})\,\mathrm{e}^{-\mathrm{i}ht}|\hat{b}_{\mathrm{s}}(\omega,\boldsymbol{\kappa}')|^2\,\mathrm{d}\boldsymbol{\kappa}\,\mathrm{d}\boldsymbol{\kappa}'\,\mathrm{d}h\,\mathrm{d}\omega}, \quad \text{(E.1)}$$

and $D(\omega,h,z,\boldsymbol{\kappa}_u,\boldsymbol{\kappa}_v,\boldsymbol{\kappa}_w)$ is defined by (B.5). By identity (B.6) we have

$$(\Delta_{\boldsymbol{\kappa}_u}+\Delta_{\boldsymbol{\kappa}_v})D(\omega,h,z,\boldsymbol{0},\boldsymbol{\kappa}_v,\boldsymbol{\kappa}_w) = \bar{D}l_x^2\mathcal{F}_1\left(\frac{\omega}{\omega_0},\frac{hL}{\bar{c}},\frac{z}{L},\boldsymbol{\kappa}_v l_x,\boldsymbol{\kappa}_w l_x\right)\mathrm{e}^{2\mathrm{i}\frac{hL}{\bar{c}}\tilde{\tau}_0(\frac{z}{L})-\bar{G}\tilde{G}_0(\frac{z}{L})},$$
$$2\nabla_{\boldsymbol{\kappa}_u}D(\omega,h,z,\boldsymbol{0},\boldsymbol{\kappa}_v,\boldsymbol{\kappa}_w) = \bar{D}l_x\mathcal{F}_2\left(\frac{\omega}{\omega_0},\frac{hL}{\bar{c}},\frac{z}{L},\boldsymbol{\kappa}_v l_x,\boldsymbol{\kappa}_w l_x\right)\mathrm{e}^{2\mathrm{i}\frac{hL}{\bar{c}}\tilde{\tau}_0(\frac{z}{L})-\bar{G}\tilde{G}_0(\frac{z}{L})},$$

with

$$\mathcal{F}_1(\tilde{\omega},\tilde{h},\tilde{z},\boldsymbol{v},\boldsymbol{w}) = \left[\Delta_{\boldsymbol{u}}+\Delta_{\boldsymbol{v}}-2\mathrm{i}\frac{\alpha}{\tilde{\omega}}\tilde{J}_0(\tilde{z})\boldsymbol{v}\cdot\nabla_{\boldsymbol{u}}-\frac{\alpha^2}{\tilde{\omega}^2}\tilde{J}_0(\tilde{z})^2|\boldsymbol{v}|^2\right]\mathcal{D}(\tilde{\omega},\tilde{h},\tilde{z},\boldsymbol{0},\boldsymbol{v},\boldsymbol{w}),$$
$$\mathcal{F}_2(\tilde{\omega},\tilde{h},\tilde{z},\boldsymbol{v},\boldsymbol{w}) = \left[2\nabla_{\boldsymbol{u}}-2\frac{\alpha}{\tilde{\omega}}\mathrm{i}\tilde{J}_0(\tilde{z})\boldsymbol{v}\right]\mathcal{D}(\tilde{\omega},\tilde{h},\tilde{z},\boldsymbol{0},\boldsymbol{v},\boldsymbol{w}).$$

In the limit $\alpha\to\infty$, we obtain by using lemma D.2

$$\frac{\mathrm{e}^{-2\mathrm{i}\frac{hL}{\bar{c}}\tilde{\tau}_0(1)+\bar{G}\tilde{G}_0(1)}}{(2\pi)^d\bar{D}\alpha^2}\int(\Delta_{\boldsymbol{\kappa}_1}+\Delta_{\boldsymbol{\kappa}_2})D(\omega,h,L,\boldsymbol{0},\boldsymbol{\kappa}+2\boldsymbol{\kappa}',\boldsymbol{\kappa})\,\mathrm{d}\boldsymbol{\kappa}$$
$$\overset{\alpha\to\infty}{\longrightarrow}\int_0^1 \Delta_{\boldsymbol{\lambda}}\check{\mathcal{B}}_{2\frac{\omega}{\omega_0}}(\tilde{z},\boldsymbol{0})\,\mathrm{e}^{-2\mathrm{i}\frac{hL}{\bar{c}}\tilde{\tau}_0(\tilde{z})}\,\mathrm{e}^{\bar{G}\tilde{G}_0(\tilde{z})}(\tilde{J}_0(1)-\tilde{J}_0(\tilde{z}))^2\,\mathrm{d}\tilde{z}$$

$$
\begin{aligned}
&- 4|\boldsymbol{\kappa}'|^2 l_x^2 \int_0^1 \check{\mathcal{B}}_{2\frac{\omega}{\omega_0}}(\tilde{z}, \mathbf{0})\, \mathrm{e}^{-2\mathrm{i}\frac{hL}{\tilde{c}}\tilde{\tau}_0(\tilde{z})}\, \mathrm{e}^{\bar{G}\tilde{G}_0(\tilde{z})} (\tilde{J}_0(1) - \tilde{J}_0(\tilde{z}))^2\, \mathrm{d}\tilde{z} \\
&+ 2\beta \int_0^1 \frac{\omega^2}{\omega_0^2} \check{\mathcal{B}}_{2\frac{\omega}{\omega_0}}(\tilde{z}, \mathbf{0})\, \mathrm{e}^{-2\mathrm{i}\frac{hL}{\tilde{c}}\tilde{\tau}_0(\tilde{z})}\, \mathrm{e}^{\bar{G}\tilde{G}_0(\tilde{z})} \\
&\times \int_{\tilde{z}}^1 \Delta_{\boldsymbol{\lambda}} \check{\mathcal{B}}_0(\tilde{z}', \mathbf{0}) [(\tilde{J}_0(1) - \tilde{J}_0(\tilde{z}))^2 + (\tilde{J}_0(\tilde{z}) - \tilde{J}_0(\tilde{z}'))^2]\, \mathrm{d}\tilde{z}'\, \mathrm{d}\tilde{z},
\end{aligned}
$$

and

$$
\begin{aligned}
&\frac{\mathrm{e}^{-2\mathrm{i}\frac{hL}{\tilde{c}}\tilde{\tau}_0(1)+\bar{G}\tilde{G}_0(1)}}{(2\pi)^{\mathrm{d}}\bar{D}\alpha} \int 2\nabla_{\boldsymbol{\kappa}_1} D(\omega, h, L, \mathbf{0}, \boldsymbol{\kappa} + 2\boldsymbol{\kappa}', \boldsymbol{\kappa})\, \mathrm{d}\boldsymbol{\kappa} \\
&\qquad \overset{\alpha\to\infty}{\longrightarrow} -4\mathrm{i}\boldsymbol{\kappa}' l_x \int_0^1 \frac{\omega}{\omega_0} \check{\mathcal{B}}_{2\frac{\omega}{\omega_0}}(\tilde{z}, \mathbf{0})\, \mathrm{e}^{-2\mathrm{i}\frac{hL}{\tilde{c}}\tilde{\tau}_0(\tilde{z})}\, \mathrm{e}^{\bar{G}\tilde{G}_0(\tilde{z})} (\tilde{J}_0(1) - \tilde{J}_0(\tilde{z}))\, \mathrm{d}\tilde{z}.
\end{aligned}
$$

Substituting these limits into (E.1) we obtain that, in the large-α regime,

$$
\begin{aligned}
R^2(t) = R_0^2 &- 2\beta\alpha^2 l_x^2 \int_{\tilde{z}(t)}^1 \Delta_{\boldsymbol{\lambda}} \check{\mathcal{B}}_0(\tilde{z}', \mathbf{0}) [(\tilde{J}_0(1) - \tilde{J}_0(\tilde{z}(t)))^2 + (\tilde{J}_0(\tilde{z}(t)) - \tilde{J}_0(\tilde{z}'))^2]\, \mathrm{d}\tilde{z}' \\
&+ 4\alpha^2 l_x^4 \frac{\int \check{\mathcal{B}}_{2\frac{\omega}{\omega_0}}(\tilde{z}(t), \mathbf{0}) \int |\boldsymbol{\kappa}'|^2 |\hat{b}_{\mathrm{s}}(\omega, \boldsymbol{\kappa}')|^2\, \mathrm{d}\boldsymbol{\kappa}'\, \mathrm{d}\omega}{\int \frac{\omega^2}{\omega_0^2} \check{\mathcal{B}}_{2\frac{\omega}{\omega_0}}(\tilde{z}(t), \mathbf{0}) \int |\hat{b}_{\mathrm{s}}(\omega, \boldsymbol{\kappa}')|^2\, \mathrm{d}\boldsymbol{\kappa}'\, \mathrm{d}\omega} (\tilde{J}_0(1) - \tilde{J}_0(\tilde{z}(t)))^2 \\
&+ 4\alpha^2 l_x^2 \frac{\int \frac{\omega}{\omega_0} \check{\mathcal{B}}_{2\frac{\omega}{\omega_0}}(\tilde{z}(t), \mathbf{0}) \int \boldsymbol{\kappa} \cdot \mathrm{Im}(\hat{b}_{\mathrm{s}} \overline{\nabla_{\boldsymbol{\kappa}} \hat{b}_{\mathrm{s}}}(\omega, \boldsymbol{\kappa}))\, \mathrm{d}\boldsymbol{\kappa}'\, \mathrm{d}\omega}{\int \frac{\omega^2}{\omega_0^2} \check{\mathcal{B}}_{2\frac{\omega}{\omega_0}}(\tilde{z}(t), \mathbf{0}) \int |\hat{b}_{\mathrm{s}}(\omega, \boldsymbol{\kappa}')|^2\, \mathrm{d}\boldsymbol{\kappa}'\, \mathrm{d}\omega} (\tilde{J}_0(1) - \tilde{J}_0(\tilde{z}(t))) \\
&- \alpha^2 l_x^2 \frac{\int \Delta_{\boldsymbol{\lambda}} \check{\mathcal{B}}_{2\frac{\omega}{\omega_0}}(\tilde{z}(t), \mathbf{0}) \int |\hat{b}_{\mathrm{s}}(\omega, \boldsymbol{\kappa}')|^2\, \mathrm{d}\boldsymbol{\kappa}'\, \mathrm{d}\omega}{\int \frac{\omega^2}{\omega_0^2} \check{\mathcal{B}}_{2\frac{\omega}{\omega_0}}(\tilde{z}(t), \mathbf{0}) \int |\hat{b}_{\mathrm{s}}(\omega, \boldsymbol{\kappa}')|^2\, \mathrm{d}\boldsymbol{\kappa}'\, \mathrm{d}\omega} (\tilde{J}_0(1) - \tilde{J}_0(\tilde{z}(t)))^2,
\end{aligned}
$$

where $\tilde{z}(t)$ is defined by (C.3). If we assume that the relative bandwidth $B \ll 1$ so that $\check{\mathcal{B}}_{2\tilde{\omega}}(\tilde{z}, \boldsymbol{\lambda}) \simeq \check{\mathcal{B}}_2(\tilde{z}, \boldsymbol{\lambda})$ for any $\tilde{\omega} \in (1 - B, 1 + B)$, then the expression of $R^2(t)$ can be simplified to

$$
\begin{aligned}
R^2(t) = R_0^2 &- 2\beta\alpha^2 l_x^2 \int_{\tilde{z}(t)}^1 \Delta_{\boldsymbol{\lambda}} \check{\mathcal{B}}_0(\tilde{z}', \mathbf{0}) [(\tilde{J}_0(1) - \tilde{J}_0(\tilde{z}(t)))^2 + (\tilde{J}_0(\tilde{z}') - \tilde{J}_0(\tilde{z}(t)))^2]\, \mathrm{d}\tilde{z}' \\
&+ 4K_0^2 l_x^4 \alpha^2 (\tilde{J}_0(1) - \tilde{J}_0(\tilde{z}(t)))^2 + 4Q_0 l_x^2 \alpha (\tilde{J}_0(1) - \tilde{J}_0(\tilde{z}(t))) \\
&- \alpha^2 l_x^2 \frac{\Delta_{\boldsymbol{\lambda}} \check{\mathcal{B}}_2(\tilde{z}(t), \mathbf{0})}{\check{\mathcal{B}}_2(\tilde{z}(t), \mathbf{0})} (\tilde{J}_0(1) - \tilde{J}_0(\tilde{z}(t)))^2.
\end{aligned}
$$

We can write $R(t)$ in terms of the original variables by using the expressions (28) for α and β, which gives (37).

Appendix F. Proof of proposition 4.3

The spectral width $K^\varepsilon(t)$ converges to $K(t)$ as $\varepsilon \to 0$, where $K(t)$ is given by

$$
\begin{aligned}
K^2(t) &= \frac{\int \cdots \int |\boldsymbol{\kappa}_1|^2 W_{(\boldsymbol{\kappa}_1,\boldsymbol{\kappa}_2),(\boldsymbol{\kappa}_1,\boldsymbol{\kappa}_4)}(\omega, t, L) \hat{b}_{\mathrm{s}}(\omega, \boldsymbol{\kappa}_2) \overline{\hat{b}_{\mathrm{s}}}(\omega, \boldsymbol{\kappa}_4)\, \mathrm{d}\boldsymbol{\kappa}_1\, \mathrm{d}\boldsymbol{\kappa}_2\, \mathrm{d}\boldsymbol{\kappa}_4\, \mathrm{d}\omega}{\int \cdots \int W_{(\boldsymbol{\kappa}_1,\boldsymbol{\kappa}_2),(\boldsymbol{\kappa}_1,\boldsymbol{\kappa}_4)}(\omega, t, L) \hat{b}_{\mathrm{s}}(\omega, \boldsymbol{\kappa}_2) \overline{\hat{b}_{\mathrm{s}}}(\omega, \boldsymbol{\kappa}_4)\, \mathrm{d}\boldsymbol{\kappa}_1\, \mathrm{d}\boldsymbol{\kappa}_2\, \mathrm{d}\boldsymbol{\kappa}_4\, \mathrm{d}\omega} \\
&= \frac{\int \cdots \int |\boldsymbol{\kappa} + \boldsymbol{\kappa}'|^2 D(\omega, h, L, \mathbf{0}, \boldsymbol{\kappa} + 2\boldsymbol{\kappa}', \boldsymbol{\kappa})\, \mathrm{e}^{-\mathrm{i}ht} |\hat{b}_{\mathrm{s}}(\omega, \boldsymbol{\kappa}')|^2\, \mathrm{d}\boldsymbol{\kappa}\, \mathrm{d}\boldsymbol{\kappa}'\, \mathrm{d}h\, \mathrm{d}\omega}{\int \cdots \int D(\omega, h, L, \mathbf{0}, \boldsymbol{\kappa} + 2\boldsymbol{\kappa}', \boldsymbol{\kappa}) |\hat{b}_{\mathrm{s}}(\omega, \boldsymbol{\kappa}')|^2\, \mathrm{e}^{-\mathrm{i}ht}\, \mathrm{d}\boldsymbol{\kappa}\, \mathrm{d}\boldsymbol{\kappa}'\, \mathrm{d}h\, \mathrm{d}\omega}.
\end{aligned} \tag{F.1}
$$

In the regime $\alpha \gg 1$ and $B \ll 1$ we obtain

$$K^2(t) = K_0^2 - 2\beta l_x^{-2} \int_{\tilde z(t)}^1 \Delta_\lambda \check{\mathcal{B}}_0(\tilde z', \mathbf{0})\, \mathrm{d}\tilde z' - \frac{\Delta_\lambda \check{\mathcal{B}}_2(\tilde z(t), \mathbf{0})}{\check{\mathcal{B}}_2(\tilde z(t), \mathbf{0})} l_x^{-2}, \tag{F.2}$$

where K_0 is the spectral width (39) of the incoming beam. Substituting the value of β we get expression (44).

Appendix G. Proof of proposition 4.4

The spatial cross correlation function $A^\varepsilon(t, \boldsymbol{x})$ has the limit $A(t, \boldsymbol{x})$ as $\varepsilon \to 0$:

$$A(t, \boldsymbol{x}) = \frac{\int \cdots \int W_{(\boldsymbol{\kappa}_1, \boldsymbol{\kappa}_2), (\boldsymbol{\kappa}_1, \boldsymbol{\kappa}_4)}(\omega, t, L)\, \mathrm{e}^{-\mathrm{i}(\boldsymbol{\kappa}_1 - \boldsymbol{\kappa}_2 + \boldsymbol{\kappa}_4)\cdot \boldsymbol{x}} \hat b_{\mathrm{s}}(\omega, \boldsymbol{\kappa}_2) \overline{\hat b_{\mathrm{s}}}(\omega, \boldsymbol{\kappa}_4)\, \mathrm{d}\boldsymbol{\kappa}_1\, \mathrm{d}\boldsymbol{\kappa}_2\, \mathrm{d}\boldsymbol{\kappa}_4\, \mathrm{d}\omega}{\int \cdots \int W_{(\boldsymbol{\kappa}_1, \boldsymbol{\kappa}_2), (\boldsymbol{\kappa}_1, \boldsymbol{\kappa}_4)}(\omega, t, L) \hat b_{\mathrm{s}}(\omega, \boldsymbol{\kappa}_2) \overline{\hat b_{\mathrm{s}}}(\omega, \boldsymbol{\kappa}_4)\, \mathrm{d}\boldsymbol{\kappa}_1\, \mathrm{d}\boldsymbol{\kappa}_2\, \mathrm{d}\boldsymbol{\kappa}_4\, \mathrm{d}\omega}$$
$$= \frac{\int \cdots \int D(\omega, h, L, \mathbf{0}, \boldsymbol{\kappa} + \boldsymbol{\kappa}', \boldsymbol{\kappa} - \boldsymbol{\kappa}')\, \mathrm{e}^{-\mathrm{i}ht} \mathrm{e}^{-\mathrm{i}\boldsymbol{\kappa}\cdot\boldsymbol{x}} |\hat b_{\mathrm{s}}(\omega, \boldsymbol{\kappa}')|^2\, \mathrm{d}\boldsymbol{\kappa}\, \mathrm{d}\boldsymbol{\kappa}'\, \mathrm{d}h\, \mathrm{d}\omega}{\int \cdots \int D(\omega, h, L, \mathbf{0}, \boldsymbol{\kappa} + 2\boldsymbol{\kappa}', \boldsymbol{\kappa})\, \mathrm{e}^{-\mathrm{i}ht} |\hat b_{\mathrm{s}}(\omega, \boldsymbol{\kappa}')|^2\, \mathrm{d}\boldsymbol{\kappa}\, \mathrm{d}\boldsymbol{\kappa}'\, \mathrm{d}h\, \mathrm{d}\omega}.$$

In the limit $\alpha \to \infty$, we obtain by using lemma D.1 that $A(t, \boldsymbol{x})$ has the form:

$$A(t, \boldsymbol{x}) = \frac{\int \frac{\omega^2}{\omega_0^2} \check{\mathcal{B}}_{2\frac{\omega}{\omega_0}}\big(\tilde z(t), \frac{\boldsymbol{x}}{l_x}\big)\, \mathrm{e}^{2\beta \frac{\omega^2}{\omega_0^2} \int_{\tilde z(t)}^1 \check{\mathcal{B}}_0(\tilde z', \frac{\boldsymbol{x}}{l_x}) - \check{\mathcal{B}}_0(\tilde z', \mathbf{0})\, \mathrm{d}\tilde z'} \big[\int \mathrm{e}^{-\mathrm{i}\boldsymbol{\kappa}'\cdot\boldsymbol{x}} |\hat b_{\mathrm{s}}(\omega, \boldsymbol{\kappa}')|^2\, \mathrm{d}\boldsymbol{\kappa}'\big]\, \mathrm{d}\omega}{\int \frac{\omega^2}{\omega_0^2} \check{\mathcal{B}}_{2\frac{\omega}{\omega_0}}(\tilde z(t), \mathbf{0}) \big[\int |\hat b_{\mathrm{s}}(\omega, \boldsymbol{\kappa}')|^2\, \mathrm{d}\boldsymbol{\kappa}'\big]\, \mathrm{d}\omega},$$

where $\tilde z(t)$ is defined by (C.3). If we also assume that the relative bandwidth $B \ll 1$, then the expression can be simplified to

$$A(t, \boldsymbol{x}) = \frac{\check{\mathcal{B}}_2(\tilde z(t), \frac{\boldsymbol{x}}{l_x})}{\check{\mathcal{B}}_2(\tilde z(t), \mathbf{0})}\, \mathrm{e}^{2\beta \int_{\tilde z(t)}^1 \check{\mathcal{B}}_0(\tilde z', \frac{\boldsymbol{x}}{l_x}) - \check{\mathcal{B}}_0(\tilde z', \mathbf{0})\, \mathrm{d}\tilde z'} \frac{\iint \mathrm{e}^{-\mathrm{i}\boldsymbol{\kappa}'\cdot\boldsymbol{x}} |\hat b_{\mathrm{s}}(\omega, \boldsymbol{\kappa}')|^2\, \mathrm{d}\boldsymbol{\kappa}'\, \mathrm{d}\omega}{\iint |\hat b_{\mathrm{s}}(\omega, \boldsymbol{\kappa}')|^2\, \mathrm{d}\boldsymbol{\kappa}'\, \mathrm{d}\omega}.$$

In the original variables, we obtain (46).

Appendix H. Proof of proposition 4.5

The spectral cross correlation function $S^\varepsilon(t, \boldsymbol{\kappa})$ has the limit $S(t, \boldsymbol{\kappa})$ as $\varepsilon \to 0$:

$$S(t, \boldsymbol{\kappa}) = \frac{\int \cdots \int W_{(\boldsymbol{\kappa}_1, \boldsymbol{\kappa}_2), (\boldsymbol{\kappa}_1 + \boldsymbol{\kappa}, \boldsymbol{\kappa}_4)}(\omega, t, L) \hat b_{\mathrm{s}}(\omega, \boldsymbol{\kappa}_2) \overline{\hat b_{\mathrm{s}}}(\omega, \boldsymbol{\kappa}_4)\, \mathrm{d}\boldsymbol{\kappa}_1\, \mathrm{d}\boldsymbol{\kappa}_2\, \mathrm{d}\boldsymbol{\kappa}_4\, \mathrm{d}\omega}{\int \cdots \int W_{(\boldsymbol{\kappa}_1, \boldsymbol{\kappa}_2), (\boldsymbol{\kappa}_1, \boldsymbol{\kappa}_4)}(\omega, t, L) \hat b_{\mathrm{s}}(\omega, \boldsymbol{\kappa}_2) \overline{\hat b_{\mathrm{s}}}(\omega, \boldsymbol{\kappa}_4)\, \mathrm{d}\boldsymbol{\kappa}_1\, \mathrm{d}\boldsymbol{\kappa}_2\, \mathrm{d}\boldsymbol{\kappa}_4\, \mathrm{d}\omega}$$
$$= \frac{\int \cdots \int D(\omega, h, L, -\boldsymbol{\kappa}, \boldsymbol{\kappa}_1 + \boldsymbol{\kappa}_2 + \boldsymbol{\kappa}, \boldsymbol{\kappa}_1 - \boldsymbol{\kappa}_2)\, \mathrm{e}^{-\mathrm{i}ht} \hat b_{\mathrm{s}}(\omega, \boldsymbol{\kappa}_2) \overline{\hat b_{\mathrm{s}}}(\omega, \boldsymbol{\kappa}_2 + \boldsymbol{\kappa})\, \mathrm{d}\boldsymbol{\kappa}_1\, \mathrm{d}\boldsymbol{\kappa}_2\, \mathrm{d}h\, \mathrm{d}\omega}{\int \cdots \int D(\omega, h, L, \mathbf{0}, \boldsymbol{\kappa}_1 + \boldsymbol{\kappa}_2, \boldsymbol{\kappa}_1 - \boldsymbol{\kappa}_2)\, \mathrm{e}^{-\mathrm{i}ht} |\hat b_{\mathrm{s}}(\omega, \boldsymbol{\kappa}_2)|^2\, \mathrm{d}\boldsymbol{\kappa}_1\, \mathrm{d}\boldsymbol{\kappa}_2\, \mathrm{d}h\, \mathrm{d}\omega}.$$

In the limit $\alpha \to \infty$, we obtain by using lemma D.1 that $S(t, \alpha^{-1}\boldsymbol{\kappa})$ has the form:

$$S(t, \alpha^{-1}\boldsymbol{\kappa}) = \frac{\iint \frac{\omega^2}{\omega_0^2} \check{\mathcal{B}}_{2\frac{\omega}{\omega_0}}(\tilde z(t), \frac{\omega_0}{\omega}(\tilde J_0(1) - \tilde J_0(\tilde z(t)))\boldsymbol{\kappa} l_x) |\hat b_{\mathrm{s}}(\omega, \boldsymbol{\kappa}_2)|^2 X(\omega, \boldsymbol{\kappa}_2)\, \mathrm{d}\boldsymbol{\kappa}_2 \mathrm{d}\omega}{\iint \frac{\omega^2}{\omega_0^2} \check{\mathcal{B}}_{2\frac{\omega}{\omega_0}}(\tilde z(t), \mathbf{0}) |\hat b_{\mathrm{s}}(\omega, \boldsymbol{\kappa}_2)|^2\, \mathrm{d}\boldsymbol{\kappa}_2\, \mathrm{d}\omega},$$

$$X(\omega, \boldsymbol{\kappa}_2) = \mathrm{e}^{\beta \frac{\omega^2}{\omega_0^2} \int_{\tilde z(t)}^1 \check{\mathcal{B}}_0(\tilde z', \boldsymbol{\kappa} l_x \frac{\omega}{\omega_0}[\tilde J_0(1) - 2\tilde J_0(\tilde z(t)) + \tilde J_0(z')]) + \check{\mathcal{B}}_0(\tilde z', \boldsymbol{\kappa} l_x \frac{\omega}{\omega_0}[\tilde J_0(1) - \tilde J_0(z')]) - 2\check{\mathcal{B}}_0(\tilde z', \mathbf{0})\, \mathrm{d}\tilde z'}$$
$$\times \mathrm{e}^{2\mathrm{i}\frac{\omega_0}{\omega}(\tilde J_0(1) - \tilde J_0(\tilde z(t)))\boldsymbol{\kappa}\cdot\boldsymbol{\kappa}_2 l_x^2},$$

where $\tilde{z}(t)$ is defined by (C.3). If we also assume that the relative bandwidth $B \ll 1$, then the expression can be simplified to

$$S(t, \alpha^{-1}\boldsymbol{\kappa}) = \frac{\check{\mathcal{B}}_2(\tilde{z}(t), (\tilde{J}_0(1) - \tilde{J}_0(\tilde{z}(t)))\boldsymbol{\kappa} l_x)}{\check{\mathcal{B}}_2(\tilde{z}(t), \mathbf{0})} \times \mathrm{e}^{\beta \int_{\tilde{z}(t)}^1 \check{\mathcal{B}}_0(\tilde{z}', \boldsymbol{\kappa} l_x[\tilde{J}_0(1) - 2\tilde{J}_0(\tilde{z}(t)) + \tilde{J}_0(z')]) + \check{\mathcal{B}}_0(\tilde{z}', \boldsymbol{\kappa} l_x[\tilde{J}_0(1) - \tilde{J}_0(z')]) - 2\check{\mathcal{B}}_0(\tilde{z}', \mathbf{0})\, \mathrm{d}\tilde{z}'} \times \frac{\iint \mathrm{e}^{2\mathrm{i}(\tilde{J}_0(1) - \tilde{J}_0(\tilde{z}(t)))\boldsymbol{\kappa}\cdot\boldsymbol{\kappa}_2 l_x^2} |\hat{b}_{\mathrm{s}}(\omega, \boldsymbol{\kappa}_2)|^2 \, \mathrm{d}\boldsymbol{\kappa}_2 \, \mathrm{d}\omega}{\iint |\hat{b}_{\mathrm{s}}(\omega, \boldsymbol{\kappa}')|^2 \, \mathrm{d}\boldsymbol{\kappa}' \, \mathrm{d}\omega}.$$

In the original variables, we obtain (48).

Appendix I. Proof of proposition 5.1

The mean reflected power observed in the relative direction $\boldsymbol{\kappa}$ is given by

$$\begin{aligned} P_{\boldsymbol{\kappa}}(t) &= \frac{1}{(2\pi)^{d+1}} \int \cdots \int W_{(\boldsymbol{\kappa}_0 + \boldsymbol{\kappa}, \boldsymbol{\kappa}_2), (\boldsymbol{\kappa}_0 + \boldsymbol{\kappa}, \boldsymbol{\kappa}_4)}(\omega, t, L) \hat{b}_{\mathrm{s}}(\omega, \boldsymbol{\kappa}_2) \overline{\hat{b}_{\mathrm{s}}}(\omega, \boldsymbol{\kappa}_4) \, \mathrm{d}\boldsymbol{\kappa}_0 \, \mathrm{d}\boldsymbol{\kappa}_2 \, \mathrm{d}\boldsymbol{\kappa}_4 \, \mathrm{d}\omega \\ &= \frac{1}{(2\pi)^{d+2}} \int \cdots \int D(\omega, h, L, \mathbf{0}, \boldsymbol{\kappa}_0 + \boldsymbol{\kappa} + \boldsymbol{\kappa}_2, \boldsymbol{\kappa}_0 + \boldsymbol{\kappa} - \boldsymbol{\kappa}_2) \\ &\quad \times \mathrm{e}^{-\mathrm{i}ht} |\hat{b}_{\mathrm{s}}(\omega, \boldsymbol{\kappa}_2)|^2 \, \mathrm{d}\boldsymbol{\kappa}_0 \, \mathrm{d}\boldsymbol{\kappa}_2 \, \mathrm{d}h \, \mathrm{d}\omega. \end{aligned}$$

If we take into account the fact that the angular aperture of the input beam is small, i.e. much smaller than $\alpha^{-1}(\omega_0 l_x/\bar{c})^{-1}$, and that it is quasi-monochromatic, i.e. $B \ll 1$, then we find that the mean reflected power observed in the relative direction $\boldsymbol{\kappa}$ is

$$P_{\boldsymbol{\kappa}}(t) = \frac{E_{\mathrm{s}}}{2\pi} \iint D(\omega_0, h, L, \mathbf{0}, \boldsymbol{\kappa}, -2\boldsymbol{\kappa}_0 + \boldsymbol{\kappa}) \, \mathrm{e}^{-\mathrm{i}ht} \mathrm{d}h \, \mathrm{d}\boldsymbol{\kappa}_0, \tag{I.1}$$

where E_{s} is the input energy defined by (35). In the large-α regime, we observe the reflected wave in a cone of angular aperture of order α^{-1} and by lemma D.2:

$$P_{\alpha^{-1}\boldsymbol{\kappa}}(t) \xrightarrow{\alpha\to\infty} \frac{\pi^d E_{\mathrm{s}} \bar{D} \bar{c} \tilde{c}_0(\tilde{z}(t))}{2L} \check{\mathcal{B}}_2(\tilde{z}(t), \mathbf{0}) \, \mathrm{e}^{\bar{G}[\tilde{G}_0(\tilde{z}(t)) - \tilde{G}_0(1)]} \times \left[1 - \mathrm{e}^{-2\beta \int_{\tilde{z}(t)}^1 \check{\mathcal{B}}_0(\tilde{z}', 0)\, \mathrm{d}\tilde{z}'} + \mathrm{e}^{2\beta \int_{\tilde{z}(t)}^1 \check{\mathcal{B}}_0(\tilde{z}', \boldsymbol{\kappa} l_x[\tilde{J}_0(1) - \tilde{J}_0(\tilde{z}')]) - \check{\mathcal{B}}_0(\tilde{z}', 0)\, \mathrm{d}\tilde{z}'}\right],$$

where $\tilde{z}(t)$ is defined by (C.3). In the original variables we obtain (49).

References

[1] Asch M, Kohler W, Papanicolaou G, Postel M and White B 1991 Frequency content of randomly scattered signals *SIAM Rev.* **33** 519–625

[2] Barabanenkov Y N 1973 Wave corrections for the transfer equation for backward scattering *Izv. Vyssh. Uchebn. Zaved. Radiofiz.* **16** 88–96

[3] Claerbout J F 1985 *Imaging the Earths Interior* (Palo Alto: Blackwell)

[4] Fante R L 1985 Wave propagation in random media: a systematic approach *Progress in Optics* vol 22 ed E Wolf (Amsterdam: Elsevier) pp 341–98

[5] Fouque J-P, Garnier J, Nachbin A and Sølna K 2006 Imaging of a dissipative layer in a random medium using a time reversal method *Monte Carlo and Quasi-Monte Carlo Methods 2004* ed H Niederreiter and D Talay (Berlin: Springer) pp 127–45

[6] Fouque J-P, Garnier J, Papanicolaou G and Sølna K 2007 *Wave Propagation and Time Reversal in Randomly Layered Media* (New York: Springer)

[7] Fouque J-P and Poliannikov O 2006 Time reversal detection in one-dimensional random media *Inverse Problems* **22** 903–22

[8] Garnier J and Sølna K 2008 Random backscattering in the parabolic scaling *J. Stat. Phys.* **131** 445–86

[9] Huang K, Papanicolaou G, Sølna K, Tsonga C and Zhao H 2005 Efficient numerical simulation for long range wave propagation *J. Comput. Phys.* **215** 448–64
[10] Ishimaru A 1978 *Wave Propagation and Scattering in Random Media* (New York: Academic)
[11] Labeyrie G, de Tomasi F, Bernard J-C, Müller C A, Miniatura C and Kaiser R 1999 Coherent backscattering of light by atoms *Phys. Rev. Lett.* **83** 5266–9
[12] Paasschens J C J 1997 Solution of the time-dependent Boltzmann equation *Phys. Rev.* E **56** 1135–41
[13] Papanicolaou G, Postel M, Sheng P and White B 1990 Frequency content of randomly scattered signals: Part II. Inversion *Wave Motion* **12** 527–49
[14] Strohbehn J W (ed) 1978 *Laser Beam Propagation in the Atmosphere* (Berlin: Springer)
[15] Tappert F 1977 The parabolic approximation method *Wave Propagation and Underwater Acoustics* ed J B Keller and J S Papadakis (Berlin: Springer) pp 224–87
[16] Thrane L, Yura H T and Andersen P E 2000 Analysis of optical coherence tomography systems based on the extended Huygens–Fresnel principle *J. Opt. Soc. Am.* A **17** 484–90
[17] Tourin A, Derode A, Roux P, van Tiggelen B A and Fink M 1997 Time-dependent coherent backscattering of acoustic waves *Phys. Rev. Lett.* **79** 3637–9
[18] van Albada M P and Lagendijk A 1985 Observation of weak localization of light in a random medium *Phys. Rev. Lett.* **55** 2692–5
[19] van Rossum M C W and Nieuwenhuizen Th M 1999 Multiple scattering of classical waves: microscopy, mesoscopy, and diffusion *Rev. Mod. Phys.* **71** 313–71
[20] White B, Sheng P, Postel M and Papanicolaou G 1989 Probing through cloudiness: theory of statistical inversion for multiply scattered data *Phys. Rev. Lett.* **63** 2228–31
[21] Wolf P E and Maret G 1985 Weak localization and coherent backscattering of photons in disordered media *Phys. Rev. Lett.* **55** 2696–9